APPLICATION OF GOOGLE EARTH ENGINE FOR RESERVOIR SEDIMENTATION ASSESSMENT: THE CASE OF TWO RESERVOIRS IN UPPER AWASH RIVER BASIN, ETHIOPIA

SAMUEL NEGUSSIE

A THESIS SUBMITTED TO THE DEPARTMENT OF WATER RESOURCES ENGINEERING

SCHOOL OF CIVIL ENGINEERING AND ARCHITECTURE

PRESENTED IN PARTIAL FULFILLMENT OF THE REQUIREMENT FOR THE DEGREE OF MASTER’S IN WATER RESOURCES ENGINEERING (SPECIALIZATION IN HYDRAULIC ENGINEERING)

OFFICE OF GRADUATE STUDIES

ADAMA SCIENCE AND TECHNOLOGY UNIVERSITY

JUNE, 2023

ADAMA, ETHIOPIA

APPLICATION OF GOOGLE EARTH ENGINE FOR RESERVOIR SEDIMENTATION ASSESSMENT: THE CASE OF TWO RESERVOIRS IN UPPER AWASH RIVER BASIN, ETHIOPIA

SAMUEL NEGUSSIE

ADVISOR(S): MULUGETA MUSSIE (Ph.D.)

A THESIS SUBMITTED TO THE DEPARTMENT OF WATER RESOURCES ENGINEERING

SCHOOL OF CIVIL ENGINEERING AND ARCHITECTURE

PRESENTED IN PARTIAL FULFILLMENT OF THE REQUIREMENT FOR THE DEGREE OF MASTER'S IN WATER RESOURCES ENGINEERING (SPECIALIZATION IN HYDRAULIC ENGINEERING)

OFFICE OF GRADUATE STUDIES

ADAMA SCIENCE AND TECHNOLOGY UNIVERSITY

JUNE, 2023

ADAMA, ETHIOPIA

DECLARATION

I hereby declare that this Master Thesis entitled "**Application of Google Earth Engine for Reservoir Sedimentation Assessment: The Case of Upper Awash River Basin, Ethiopia**" is my original work. That is, it has not been submitted for the award of any academic degree, diploma, or certificate in any other university. All sources of materials that are used for this thesis have been duly acknowledged through citation.

Samuel Negussie ____________________ ______________

Name of the student Signature Date

RECOMMENDATION

I, the advisor(s) of this thesis, hereby certify that I have read the revised version of the thesis entitled "**Application of Google Earth Engine for Reservoir Sedimentation Assessment: The Case of Upper Awash River Basin, Ethiopia**" prepared under my/our guidance by **Samuel Negussie** submitted in partial fulfillment of the requirements for the degree of Mater's of Science in Water resources engineering (specialization in Hydraulic engineering). Therefore, I recommend the submission of a revised version of the thesis to the department following the applicable procedures.

Mulugeta Mussie (Ph.D.)	______________________	_______________
Major Advisor	Signature	Date
_________________________	______________________	_______________
Co-advisor	Signature	Date

APPROVAL PAGE

I, the advisor of the thesis entitled "**Application of Google Earth Engine for Reservoir Sedimentation Assessment: The Case of Upper Awash River Basin, Ethiopia**" and developed by Samuel Negussie, hereby certify that the recommendation and suggestions made by the board of examiners are appropriately incorporated into the final version of the thesis.

Mulugeta Mussie (Ph.D.)	____________________	______________
Major Advisor	Signature	Date
____________________	____________________	______________
Co-advisor	Signature	Date

We, the undersigned, members of the Board of Examiners of the thesis by **Samuel Negussie** have read and evaluated the thesis entitled "**Application of Google Earth Engine for Reservoir Sedimentation Assessment: The Case of Upper Awash River Basin, Ethiopia**" and examined the candidate during open defense. This is, therefore, to certify that the thesis is accepted for partial fulfillment of the requirement of the degree of Master of Science in Water resources Engineering (specialization in Hydraulic Engineering).

______________________	______________________	______________________
Chairperson	Signature	Date
______________________	______________________	______________________
Internal Examiner	Signature	Date
______________________	______________________	______________________
Eternal Examiner	Signature	Date

Finally, approval and acceptance of the thesis is contingent upon submission of its final copy to the Office of Postgraduate Studies (OPGS) through the Department Graduate Council (DGC) and School Graduate Committee (SGC).

______________________	______________________	______________________
Department Head	Signature	Date
______________________	______________________	______________________
School Dean	Signature	Date
______________________	______________________	______________________
Office of Postgraduate Studies	Signature	Date

ACKNOWLEDGEMENT

I would like to express my deepest appreciation and gratitude to everyone who has supported and guided me throughout the journey of conducting this thesis. First and foremost, I would like to thank my advisor, Mulugeta Mussie (Ph.D.), for his unwavering guidance, patience, and encouragement. His vast knowledge, expertise, and enthusiasm for research have inspired me to delve deeper into my chosen topic and strive for excellence.

I also thank Dereje Birhanu (Ph.D.) for sharing his valuable insights, meticulous attention to detail, and willingness to provide assistance when needed.

I would like also to thank the Ministry of Water and Energy and Addis Abba Water Supply and Sewerage authority for their cooperation in availing the necessary data.

I extend my heartfelt gratitude to my fellow researchers and colleagues, for their camaraderie, intellectual stimulation, and friendship during this collaborative effort.

My sincerest thanks go to my family, for their unwavering love, support, and belief in my abilities. Their constant encouragement and sacrifices have provided me with the motivation and strength needed to complete this thesis.

Finally, I would like to thank Adama Science and Technology University(ASTU), for their contribution to my research in various ways.

This thesis would not have been possible without the support of all the individuals mentioned above, and I am eternally grateful for their assistance in bringing this project to fruition.

TABLE OF CONTENTS

LIST OF TABLES

LIST OF FIGURES

LIST OF ABBREVIATION AND ACRONYMS

API	Application programming interface
AAWSSA	Addis Ababa Water Supply and Sewerage Authority
CPUs	Central Processing Unit
ECDSWC	Ethiopian Construction Design and Supervision Works Corporation
EEP	Ethiopian Electric Power
ETM	Enhanced Thematic Mapper
FSL	Full supply level
GEE	Google earth engine
GIS	Geographical information system
GPS	Geographical Information System
GPUs	Graphics Processing Units
m.a.s.l	Mean above sea level
MDDL	Minimum Drawdown Level
MoWE	Ministry of Water and Energy
NDWI	Normalized Difference Water Index
OLI	Operational Land Manager
RGB	Red Green Blue
RL	Reservoir Level

ABSTRACT

Globally reservoirs are experiencing severe problems of sedimentation, which have resulted in reduced storage capacity, increased flood risks, and reduce the integrity of dams. Accordingly, the consequences of sedimentation cause several economic, social, and environmental problems. Therefore, it became essential to evaluate sediment accumulation in all reservoirs. Various methods and techniques have been used to analyze sediment deposits in these reservoirs. Among these methods, the satellite remote sensing technique has proven to be an effective. Nevertheless, accurate and automated methods for calculating the reservoir storage capacity using satellite imagery are not yet available. Therefore, the present study developed an automated methodology using Google Earth Engine to assess reservoir sedimentation and applied it on Koka and Gefersa I/II reservoirs located in the upper Awash River Basin. The capability of the Google Earth Engine (GEE) for the assess reservoir sedimentation was then examined by comparing its results with those of recent bathymetric surveys. Landsat imagery, reservoir water level data, pre-impoundment reservoir capacity and bathymetry survey data, were utilized. The storage capacity of the Koka reservoir between the MDDL 1583.54 m.a.s.l and FSL 1590.6 m.a.s.l was estimated to be 1044 Mm^3 *for the year 2021-2022. It was then compared to the original live storage capacity, and there is a loss of 606* Mm^3 *live storage capacity within a period of 60 years (from 1960 to 2021). Thus, the average annual loss was 10.1* Mm^3 $year^{-1}$*(0.97 %). Similarly, the storage capacity of Gefersa I/II between MDDL 2580.01 m.a.s.l and FSL 2587.11 m.a.s.l was estimated to be 8.102* Mm^3 *for the year 2021/2022. It was then compared to the original live storage capacity, and there is a loss of 0.398* Mm^3 *live storage capacity. Thus, the average annual loss was* 0.007 Mm^3 $year^{-1}$ *(0.08%). The findings revealed that the result found from GEE is in agreement with the results of the bathymetry. In addition, P-test and T-test results showed there is there is a close correspondence between the bathymetry survey result and GEE result for both reservoirs. Therefore, results demonstrated the effectiveness of utilizing Google Earth Engine as a powerful tool in monitoring and analyzing reservoir sedimentation.*

Key word: Reservoir sedimentation, remote sensing, Google Earth Engine

1 INTRODUCTION

1.1 Background

The construction of dams to create artificial water storage systems is crucial for maintaining the sustainability and well-being of communities, as they provide a reliable water source for drinking, agriculture, and energy production. Additionally, these reservoirs offer a range of recreational activities, support navigation, and safeguard downstream valleys from extreme floods and droughts. Nevertheless, sedimentation becomes a major issue, resulting in reduced storage capacity and directly affecting the reservoir's future performance (Negm et al., 2017).

Sediment accumulation in reservoirs is a problem experienced by dams, which cannot be quantified at its origin and occurs in the catchment of the reservoirs (Ninija Merina, 2016). In general, soil erosion is the main reason of reservoir sedimentation, which involves the transportation of soil particles, resulting from the process of erosion in the catchment area, by flowing water or other media. These particles subsequently settle in layers within water bodies such as reservoirs and rivers by forming solid deposits (Obialor et al., 2019). The sediment transported by moving water or streams into the reservoir starts to accumulate and is deposited on the reservoir floor at various depths. First, the larger particles settle, followed by finer particles that remain suspended and may eventually settle at the bottom of the reservoir. Some of these finer materials can also pass over the spillway or through outlets to the downstream side of the dam. (Avinash & Chandramouli, 2018).

It is widely documented that dams constructed on rivers experience sedimentation. This process depends on various natural and human-induced factors (Obialor et al., 2019). As a natural process, streams and rivers in a catchment are continuously provided with sediment due to factors related to the catchment’s geology, geomorphology, hydrogeology and soil characteristics. On the other hand, human activities and interference in the upstream watershed led to faster sediment accumulation in the reservoirs. Factors like rapid population growth, deforestation, improper land cultivation, and unregulated overgrazing primarily in developing countries contribute to this accelerated soil erosion (Foteh et al., 2018).

Globally, around 40,000 large reservoirs experience sedimentation issues, and it is estimated that every year, between 0.5% - 1% of their total storage capacity is lost due to this problem (Schleiss, 2013). Similarly, in Ethiopia there are various reservoirs being constructed, such as the Grand Ethiopian Renaissance Dam (GERD), as well as numerous operational reservoirs. These reservoirs are utilized for the nation's development by federal and regional governments. However, the country has faced challenges in managing reservoir sedimentation due to various factors over several decades (Geleta, 2011). As a result, most of the reservoirs have experienced sedimentation problems such as the Gefersa and Koka reservoirs. Thus, direct and indirect impacts of sedimentation are leading to various economic, social, and environmental issues.

Therefore, these problems make reservoir sedimentation an active and expanding field of research (Schleiss, 2013). Consequently, the findings gained from these researches can assist in determining the existing live storage capacity of reservoirs, ensuring effective management of water resources, and facilitating timely catchment area treatment if necessary. There are several methods and techniques available for the assessment of sediment deposited in the reservoir such as empirical models, hydrographic survey, model studies, mathematical models, data-driven models, Stream flow analysis, artificial intelligence, conducting surveys, satellite remote sensing, and Area Reduction method (Wagh & Manekar, 2021).

Among these methods, remote sensing technology has been employed for a long period to determine the water-spread area, which is then used to estimate the capacity of the reservoir (Singh et al., 2018). This method enables data acquisition over a long duration and wide spectral range, making it superior from traditional data acquisition approaches. The spatial, spectral, and temporal characteristics of remote sensing data offer invaluable and up-to-date comprehensive information on changes in the reservoir's water-spread area as well as sediment deposition and distribution patterns within the reservoir(Wagh & Manekar, 2021). Furthermore, it offers a reasonably cost-efficient and timely approach for evaluating reservoir sedimentation during the operational phase. As a result, recent studies have determined that remote sensing is an effective technique for monitoring surface water resources.

However, an accurate and automated methodology for determining the reservoir storage capacity using satellite imagery is not yet available. In addition, there are obstacles associated with utilizing large amounts of satellite imagery related to their treatment, acquisition, visualization, and storage (Condeça et al., 2022). For these matter , Google Earth Engine(GEE) platform can be utilized to assess the temporal change in the water spread area and can analyze efficiently to evaluate the pattern of sediment deposition in a reservoir (Singh et al., 2018).

The GEE platform serves as an online application, providing an API (Application Programming Interface) that offers an access to computational resources and satellite imagery. This system greatly reduces users' reliance on their own computing resources and data acquisition, which can be sometime difficult to acquire. With GEE, individuals can utilize and process data on a programming platform through JavaScript and Python, thereby empowering the way scientists, researchers, and communities analyze information, produce trend maps, and pinpoint resources on the Earth's surface. In addition, this platform enhances the accuracy of surface detection and mapping over extensive areas. Furthermore, it eliminates the need for high-performance computing devices or software. GEE provides the ability to rapidly analyze and categorize satellite data, enabling highly relevant and precise outcomes to be achieved.

Several studies have been done in the past related to reservoir sedimentation (Avinash & Chandramouli, 2018; Foteh et al., 2018; Ninija Merina, 2016; Wagh & Manekar, 2021). However, very few studies have been conducted on the assessment of reservoir capacity using this platform. For this reason, the present study used the GEE platform to develop an automatic methodology to assess sediment accumulation in a reservoir.

1.2 Problem Statement

Reservoirs play a vital role in water resource management, especially in arid and semiarid regions. However, reservoir sedimentation is a significant issue that affects their functionality and lifespan. Sedimentation reduces water storage capacity, increases flood risks, and reduce the integrity of dams. Therefore, it is essential to determine sediment accumulation in all reservoirs. Thus, by using the obtained information, it is possible to determine the existing live storage capacity of the reservoir, allowing for effective water resource management and timely implementation of treatment, if necessary, in the catchment area (Perera et al., 2023; Rohi & Bisri, 2013)

Various tools and methods have been developed to assess reservoir sedimentation, and numerous studies have been conducted worldwide to address the issues associated with it by employing different methods(Pandey et al., 2016). Among them, the use of remote sensing techniques has significantly improved the efficiency and convenience of quantifying sedimentation in reservoirs as well as assessing its distribution and silt deposition patterns. This approach is very cost-effective and time-efficient compared to traditional methods. This trend is expected to continue because of the increased accessibility of more open-access remote sensing data and the continuous progress in sensor, image processing, and computer vision technologies(Tesfaye et al., 2022).

Unfortunately, fully utilization of these resources demands significant technical expertise, accessibility, and resources. In addition, there are obstacles associated with utilizing of these images related to their acquisition, treatment, storage, and visualization (Condeça et al., 2022). A major obstacle involves having a fundamental understanding of information technology (IT) management, data acquisition and storage, as well as using various geospatial data processing frameworks (Gorelick et al., 2017). Furthermore, precise and automatic methodologies utilizing satellite imagery to quantify reservoir volumes are lacking. Most research papers on reservoir sedimentation assessment heavily rely on sophisticated remote sensing software, such as the Environment for Visualizing Images (ENVI) and the Earth Resources Data Analysis System (ERDAS) Imagine.

Nevertheless, utilizing the Google Earth Engine as a remote sensing tool can address these problems. As a cloud-based platform for big geo-data analysis, GEE provides researchers with unparalleled access to remote sensing data and analytical tools, reducing the challenges associated with data acquisition and processing. Moreover, it offers a cost-effective solution for researchers in developing countries, which often suffer from scarce data sources and limited financial resources (Kumar & Mutanga, 2018). Furthermore, the use of GEE enables scientists to remotely assess sedimentation in hard-to-reach locations that are otherwise difficult to study.

The Google Earth Engine (GEE) has been utilized in various research fields for different purposes. However, very few studies have been conducted on the evaluation of reservoir capacity using GEE as a tool. Consequently, the current study investigated the feasibility of using the GEE platform by developing an automated methodology for assessing reservoir sedimentation and examining its capability. Accordingly, this study evaluated reservoir sedimentation using the Google Earth Engine platform and compared the findings with bathymetry survey data. By examining the capability of GEE for reservoir sedimentation study, it can serve as a baseline record for others who are involved in assessing reservoir sedimentation using GEE.

1.3 General Objective

The main objective of this study was to develop an automated methodology utilizing Google Earth Engine for assessing reservoir sedimentation

1.3.1 Specific Objective

- To apply this methodology on Koka and Gefersa I/II reservoirs to estimate the sediment deposited in these reservoirs.
- To develop revised area elevation capacity curve of Koka and Gefersa I/II reservoirs.
- To explore the effectiveness and capabilities of the Google Earth engine to assess reservoir sedimentation by comparing the results with bathymetry data.

1.4 Research Questions

- How much storage capacity is lost due to sedimentation in Koka and Gefersa I/II reservoir?
- What is the present storage capacity of the Koka and Gefersa I/II reservoirs?
- Is the Google Earth engine suitable for assessing sediment deposition in reservoirs?

1.5 Significance of the study

Sedimentation in reservoirs is a global phenomenon that involves the transport, deposition, and build-up of sand and sediment within these water bodies(Obialor et al., 2019). This phenomenon can lead to significant economic impacts, potentially affecting water resources, energy provision, flood management, and fish inhabitants. In particular, sediment accumulation can reduce the storage capacity of reservoirs, leading to increased flood risks and decreased power generating efficiency as turbine passages are filled with materials that reduce the water flow velocity(Wagh & Manekar, 2021).

To effectively manage and operate reservoirs, understanding sediment deposition is crucial. Periodic evaluations of reservoir sedimentation are necessary. Therefore, it is essential to create an automated approach that can assist engineers, scientists, policymakers, NGOs, field workers, and even the general public with minimal effort, expense, and time

Therefore, the present study has a significant contribution in understanding the sediment deposition in a reservoir by using the Google earth engine with high accuracy of surface detection and mapping across large areas. In addition, by validating the effectiveness of GEE in reservoir sedimentation assessments and promoting its adoption, this study contributes to a better understanding and provides insights to encourage its broader usage in reservoir sedimentation assessment.

Moreover, the code developed for the present study is accessible on GitHub and through the link provided in third chapter. This ensures that users, regardless of their programming expertise, can access and utilize the code for studying reservoir sedimentation. This will make it easier to conduct future sedimentation studies on different reservoirs.

In general, this research has significant implications for the active management of reservoir sedimentation, especially in developing countries, where resources are often limited. In addition, using modern high technology, such as GEE, can encourage other researchers to familiarize themselves with this cloud computing platform and leverage its capabilities in their own research, leading to further advancement in the field of remote sensing and water resources.

1.6 Scope and Limitation of the study

The scope of this study is to develop an automated methodology utilizing Google Earth Engine for assessing reservoir sedimentation and apply it to Koka and Gefersa I/II reservoirs to estimate the sediment deposited in these reservoirs. Additionally, the study aims to develop revised area elevation capacity curves of Koka and Gefersa I/II reservoirs. The effectiveness and capabilities of the Google Earth engine to assess reservoir sedimentation will be explored by comparing the results with bathymetry data. The study will contribute to the development of an automated approach that can assist engineers, scientists, policymakers, NGOs, field workers, and the general public with minimal effort, expense, and time.

The study will be limited by the availability and quality of the data used. The accuracy of the results will depend on the quality of the remote sensing imagery used to estimate the sediment deposited in the reservoirs. Additionally, the study will be limited to the Koka and Gefersa I/II reservoirs, and the results may not be generalizable to other reservoirs. The study will also be limited by the assumptions made in the methodology used to estimate sediment deposition.

1.7 Organization of the thesis

The thesis is organized into five chapters. Chapter one provides an introduction to the study, including the background, problem statement, general and specific objectives, research questions, significance, and scope of the study. Chapter two presents a literature review on reservoir sedimentation, including an overview of the concept, sedimentation process, causes, impacts, assessment methods, and the use of Google Earth Engine as a remote sensing tool. Chapter three describes the materials and methods used in the study, including the study area, data and tools used, and the methodology flow chart. Chapter four presents the results and discussion, including the estimated water spread area and volume of the reservoirs, and a discussion of the findings. Finally, Chapter five provides the conclusion of the study.

2 LITERATURE REVIEW

2.1 Reservoir sedimentation an overview

2.1.1 General concept of reservoir sedimentation

Dams are constructed worldwide to obstruct or control the flow of water by creating a large reservoir. A dam built on a stream channel affects the hydraulic properties of the flow and its capability to transfer sediment through the fluvial system. The equilibrium between sediment inflow and outflow is dramatically altered by the construction of dams, which creates an impounded river reach characterized by extremely low flow velocities and efficient sediment trapping (Jain & Singh, 2003). Sediments transported by the river system mainly settle in a reservoir as a result of decreased velocity because the reservoir's width is significantly larger than that of the river channel. Simultaneously, the water turbulence diminished. These factors cause the flow to be incapable of carrying all the sediment particles, leading to their deposition.

Therefore, reservoir sedimentation refers to the process of filling a reservoir behind a dam with material brought in by the fluvial system. In addition, according to Schleiss et al. (2013) Reservoir sedimentation can be defined as the process by which reservoirs accumulate sediment until they eventually become completely filled. Water flowing from a catchment upstream of a reservoir has the potential to erode the catchment area and deposit debris either upstream or within the reservoir (Obialor et al., 2019).

2.1.2 Causes of reservoir sedimentation

All reservoirs are subjected to sedimentation. Typically, soil erosion is the main cause of reservoir sedimentation. Erosion refers to the process through which soil or rock materials are loosened or dissolved, leading to their removal from any area on the Earth’s surface (Jain & Singh, 2003). Erosion-derived soil particles within a catchment are disseminated by river currents and can be found in streams, gullies, and river basins. Soil erosion is a complex process that depends on both natural and anthropogenic factors (Obialor et al., 2019). Sediment from inherent sources like the catchment's geology, geomorphology, hydrogeology, and soil attributes continuously fill rivers and streams. In addition, human activities and interference in the upstream watershed led to faster sediment accumulation in the reservoirs. Factors like rapid population growth, deforestation, improper land cultivation, and unregulated overgrazing primarily in developing countries contribute to this accelerated soil erosion (Foteh et al., 2018).

Most sediments are carried into reservoirs by streams as a result of soil erosion. These sediments can originate from the far, middle, and near reaches of the watershed and inside the reservoir itself (Schleiss, 2013). The far-reach consists of sediment produced on the steep slopes of valleys due to soil erosion and rock weathering, as well as unchanneled transport by water and wind. Middle-reach sediment sources encompass rills, gullies, stream bank erosion, and legacy loads. Lastly, sediment generated within the reservoir primarily comes from direct contributions of landslides above and below water, stemming from the reservoir banks and underwater slopes.

A reservoir receives all of the eroded sediment particles that a watershed produces as a result of soil erosion. In reservoir sediment particles progressively settle due to gravity and consolidate over time as a reservoir loses energy due to a decrease in velocity. To address the issue of sediment accumulation in reservoirs due to erosion from the catchment area, efforts have been made to connect soil erosion, sediment yield, and reservoir sedimentation, as these factors directly or indirectly impact the lifespan of the reservoir. (Dutta, 2016).

2.1.3 Impacts of reservoir sedimentation

The issue of sedimentation affects storage dams across the globe. Effective strategies to manage sediment are crucial, as, over time, such buildup can lead to severe complications. Among these are reduced reservoir storage capacity, which hampers the ability to regulate water flow. This, in turn, has wide-ranging effects on aspects such as water supply, flood control, hydropower, navigation, recreational activities, and environmental benefits, all of which depend on water release from these storage facilities(Sumi & Hirose, 2009; Mohammad, 2020). Along with storage loss, a numerous of sediment-related issues may surface both upstream and downstream of dams. Sediment interaction can hinder water usage for its designated purposes. Intake blockages and increased abrasion rates of hydraulic equipment are examples of sediment causing disruptions, leading to higher maintenance costs. Furthermore, disruptions in the upstream channel may extend over vast distances above the reservoir, potentially increasing the flood risks in these regions. The combined effects of sediment trapping and flow regulation can also significantly impact the ecology, water clarity, sediment equilibrium, nutrient distribution, and overall shape of the river (Sumi & Hirose, 2009).

2.1.4 Reservoir sedimentation in Ethiopia

The construction of reservoirs in Ethiopia serves essential purposes such as providing water supply, generating hydropower, supporting irrigation, and controlling floods. Nonetheless, the country faces significant challenges due to excessive sedimentation, particularly because it experiences severe overland soil erosion and has limited resources to tackle this issue (Haregeweyn et al., 2006). This sedimentation problem is primarily caused by the country's rivers, which carry enormous sediment loads and contribute to the issue (Gurmu et al., 2021). Consequently, this issue is prevalent in Ethiopian reservoirs, causing many to lose their storage capacity and negatively affecting water quality.

The rapid accumulation of sediments in Ethiopian reservoirs, which are designed to provide hydroelectric power and irrigation water, has resulted in the loss of these critical services and considerable investments made in their establishment (Moges et al., 2018). Many hydropower and irrigation reservoirs in the country, such as Legedadi, Abasamuel, Angerib, Borkena, Tekeze, Gilgel Gibie I, Koka, and others, have faced issues with sediment buildup (Tsegaye & Bharti, 2021). Furthermore, there are severe instances of sedimentation in Ethiopia, like the Borkena Dam in South Wollo, which incurred a cost of US$ 35 million in 1991, and the Adrako Dam (Ebinat, South Gondar), where the dead storage volumes of the reservoirs were filled with silt before construction was even finished (Haregeweyn et al., 2006). This issue not only raises the costs of maintaining water distribution systems but also adversely affects downstream crop yields by blocking irrigation channels.

This indicates that sedimentation is a major issue in Ethiopia's reservoirs. The current state of previously built reservoirs reveals a considerable annual loss in storage capacity owing to sediment accumulation. To ensure the sustainability of water resource projects, it is crucial to focus on watershed management activities that address erosion, river banks, and reservoir sedimentation (Geleta 2011). However, there is a lack of sufficient research or data on reservoir sedimentation in the country, which makes it difficult to accurately determine the current storage capacity of these reservoirs for effective and efficient management (Adugna & Cherie, 2021).

2.2 Reservoir sedimentation assessment methods

Repeated reservoir capacity surveys play a crucial role in determining the total volume occupied by sediment, sedimentation patterns, and shifts in the stage-area and stage-storage curves. Consequently, various sedimentation assessment methods have been developed and employed after dam construction. Some of the widely used methods include Empirical and Mathematical models, the inflow–outflow method, hydrographic/bathymetric surveys, and Satellite Remote Sensing (SRS) techniques.

Empirical methods and mathematical models are commonly used during the planning stages of reservoir sedimentation predictions. The other methods are primarily used for monitoring sedimentation during the operation phases. Streamflow analysis requires daily measurements of water and sediment flows upstream and downstream of reservoirs, starting on the day of reservoir impoundment. While hydrographic surveys are costly, time-consuming, and cannot be regularly conducted at short intervals. Nevertheless, the availability of free and publicly accessible satellite data has opened new monitoring possibilities in previously inaccessible areas.

In the recent past, the availability of multispectral satellite data obtained through remote sensing for reservoir capacity studies has expanded (Pandey et al. 2016). This technique enables data acquisition over an extended period and wide spectral range, making it superior to traditional data acquisition methods (Avinash & Chandramouli, 2018; Foteh et al., 2018). Satellite data offers several advantages over conventional sampling techniques, such as repetitive coverage of a specific area every few weeks, a comprehensive view that is unattainable with traditional methods, and almost immediate spatial data for areas of interest. Analyzing remote sensing data proves to be more economical and time-saving compared to traditional techniques. (Jain & Singh, 2003). The spatial, spectral, and temporal characteristics of satellite data provide valuable and timely information about the water spread area.

This approach has proven to be highly effective and convenient for measuring sedimentation in reservoirs and for evaluating their distribution and silt deposition patterns. Combining remote sensing technology with a geographic information system (GIS) provides spatial, temporal, and spectral data, which aids in analyzing sediment distribution patterns within reservoirs. This method not only allows us to identify water spread area at different reservoir levels but also assists in creating an updated area-capacity curve (Foteh et al., 2018). The water spread area of the reservoir for a particular reservoir elevation can be obtained accurately from satellite data. The reduction in the water spread area for a particular reservoir elevation indicates sediment deposition at that level. Later, the variation between the initial and updated area-elevation-capacity curves indicated the reservoir's capacity loss caused by sedimentation(Wagh & Manekar, 2021; Ninija Merina, 2016).

The evaluation of reservoir sedimentation has greatly benefited from the advancements in remote sensing technology. This progress is likely to continue as open-access remote sensing datasets become more readily available, and sensor, image processing, and computer vision technologies keep evolving. Recent studies have demonstrated the effectiveness of remote sensing in monitoring surface water resources. This topic tried to explore recent research papers on reservoir sedimentation assessment utilizing remote sensing techniques.

Wagh and Manekar (2021) utilized remote sensing methods to assess sedimentation in the Ujjani reservoir and proposed desilting strategies. They estimated sediment volume by measuring water-spread area using satellite imagery and employed the modified normalized difference water index (MNDWI) method. Avinash and Chandramouli (2018) conducted a similar analysis at the Kabini Reservoir using satellite data and determined the water spread area for different water levels. Jain, Singh, and Seth (2002) evaluated sediment deposition in the Bhakra Reservoir using remote sensing and analyzed satellite data to estimate sediment amounts. Negm et al. (2017) employed remote sensing and GIS to evaluate reservoir storage capacity decrease in AHDR active and inactive zones. They derived water spread area from satellite imagery and estimated sediment volume using remote sensing/GIS methods.

Numerous research papers have explored the assessment of reservoir sedimentation using remote sensing techniques, demonstrating the growing interest in this modern approach. While remote sensing has shown promise as an innovative solution for reservoir sediment monitoring and management. However, it is difficult for researchers and practitioners face when attempting to employ remote sensing techniques. These challenges include data accuracy, accessibility, and technical expertise, underscoring the need for further advancements and adaptations to overcome barriers to their effective utilization in this field.

2.3 Google Earth Engine as a Remote sensing tool

2.3.1 Explanation and Development of GEE

Advances in satellite imagery technologies have increased and become freely available from various U.S. Government agencies including NASA, the U.S. Geological Survey, and NOAA, as well as the European Space Agency, and a wide variety of tools have been developed to facilitate large-scale processing of geospatial data. Unfortunately, fully utilizing these resources requires a considerable amount of technical expertise, accessibility, and resources.

One major obstacle is the knowledge of basic information technology (IT) management, which encompasses data acquisition and storage, parsing obscure file formats, managing databases, machine allocations, job and queue management, CPUs, GPUs, networking, and utilizing any of the various geospatial data processing frameworks (Gorelick et al., 2017). Due to this burden, many academics and operational users may not be able to use these tools, which would limit access to the data present in many big remote-sensing datasets to remote-sensing specialists. In order to offer a comprehensive solution that addresses various present and future challenges and needs in remote sensing applications, it is crucial to create a secure, effective, and cutting-edge cloud computing platform (Chi et al., 2016).

Cloud computing platforms offer efficient methods for storing, accessing, and analyzing datasets on robust servers, effectively transforming them into virtual supercomputers for users. These systems deliver infrastructure, platforms, storage services, and software packages in various ways to meet user needs (Chi et al. 2016). Several cloud computing platforms are currently available, such as Amazon Web Services (AWS), Microsoft's Azure, and Google Earth Engine (GEE), which was introduced by Google in 2010.

Google Earth Engine is a cloud-based platform designed for planetary-scale geospatial analysis, leveraging Google's vast computational power to address various pressing societal issues (Gorelick et al., 2017). This platform excels in tackling big data analysis challenges, such as processing enormous amounts of data at high speeds. Numerous studies have utilized GEE data for geospatial analysis in various applications on local and global scales (Tamiminia et al., 2020). Compared to other cloud computing platforms, Google Earth Engine simplifies the use of high-performance computing for the management of large geospatial datasets without dealing with typical IT problems. Additionally, GEE is accessible to everyone, easy for developing algorithms, and allows for batch processing of image processing tools (Amani et al., 2020).

2.3.2 Key features and capabilities

The features of GEE have been discussed in many works of literature. However, recent literature has categorized the essential characteristics of GEE as follows:

I. Computational Resources

Google Earth Engine (GEE) offers vast amounts of public remote sensing imagery and other ready-to-use products, along with a user-friendly explorer web application. This incredible resource offers researchers access to an extensive selection of public datasets, including a remote sensing archive containing petabytes of cloud-stored data. With coverage ranging from local to global scales and across multiple time periods, GEE presents an unrivaled opportunity for researchers to perform studies with minimal costs and equipment requirements (Kumar & Mutanga, 2018). Moreover, GEE allows users to upload and analyze their own images and data, utilize pre-processed images, and benefit from its data storage capabilities – thereby opening up numerous possibilities for research projects across the globe (Tamiminia et al., 2020).

II. High-Speed Computation

The GEE platform leverages Google's powerful computing infrastructure to enable parallel processing of geospatial data, significantly reducing computation time. By utilizing cloud computing capabilities, GEE allows the processing of massive amounts of image and vector data without the need to store or analyze it on a local computer. This facilitates fast parallel processing and the implementation of machine learning algorithms using Google's advanced computational resources.

III. Application Programming Interfaces (APIs)

GEE offers a library of Application Programming Interfaces (APIs) with development environments compatible with widely-used programming languages like JavaScript and Python. Its data accessibility, computing infrastructure, programming capabilities, API reference documentation, and Git-based script management can inspire both experts and those with limited programming skills to utilize GEE for their applications. (Tamiminia et al., 2020).

These essential features allow users to explore, examine, and visualize geospatial big data effectively without requiring supercomputers or specific coding skills. Earth Engine is crafted with the purpose of effortlessly facilitating the exchange of findings between scientists, policymakers, non-profit organizations, field personnel, and the wider community. It doesn't demand proficiency in application creation, website coding, or HTML for users to develop interactive tools or produce structured data outcomes once an algorithm has been established using Earth Engine (Amani et al., 2020a).

2.3.3 Applications of Google Earth Engine (GEE)

For the reason that, its capabilities of dealing with big data analysis challenges, the GEE has been applied in different research areas for different purposes. Some of the applications of GEE, including Land Use/Land Cover Change, Mapping irrigated cropland, Forest mapping , Flood Mapping ,Drought monitoring, Crop yield estimation, Evapotranspiration, Wetland Mapping, Species habitat monitoring, Disease risk mapping, Natural hazard management and etc.

Mapping surface water is another application of GEE. It has been widely utilized for the mapping, detection, and monitoring of surface water. Zilong et al. (2020) used GEE for surface water mapping and revealed that the platform can achieve greater accuracy and efficacy in a complex water environment when compared to traditional methodologies. Similarly, Nghia et al. (2022) used GEE to monitor and map the flooding across the study area, and GEE proved to be an admirable platform. The same author suggested GEE to monitor the flood in other areas.

Tamiminia et al. (2020) analyzed 349 studies that utilized Google Earth Engine (GEE) as a tool for geo-big data analysis in various remote sensing applications, subsequently categorizing them into different groups. Similarly, Amani et al. (2020) examined 450 GEE-related journal articles to determine the primary disciplines, and subsequently divided the papers into different categories representing their main applications. A significant number of these studies applied GEE in vegetation and forest monitoring as well as land cover/use change mapping (Kumar & Mutanga 2018). As a result, the major applications of GEE can be categorized as

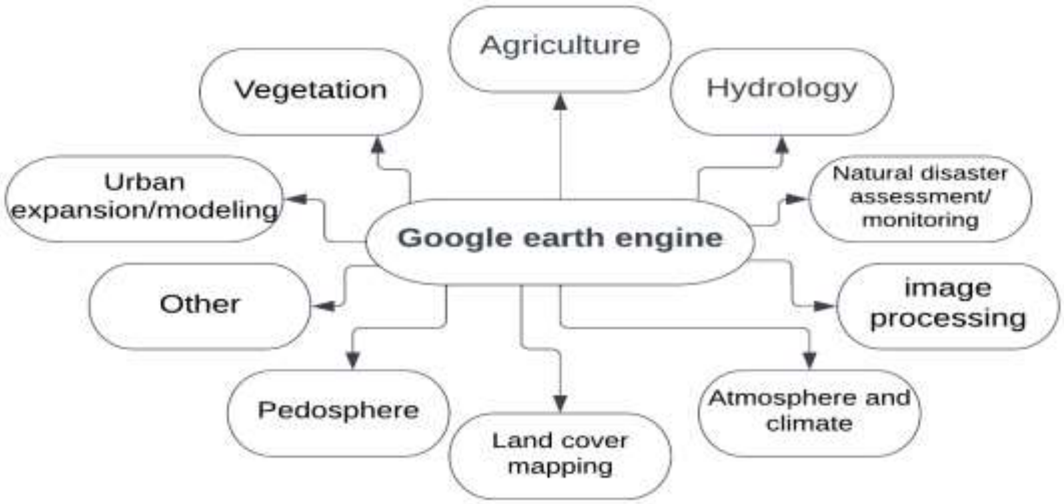

Figure 2-1 Application of Google Earth Engine (GEE)

2.4 Reservoir sedimentation assessment using GEE as a tool

For reservoir sedimentation assessment users do not have to entirely relay on specialist remote sensing software, such as Environment for Visualizing Images (ENVI) and Earth Resources Data Analysis System (ERDAS) Imagine. Using Google Earth Engine (GEE), reservoir sedimentation can be estimated, and the platform allows for analyzing temporal changes in water spread area to understand the sediment deposition pattern in a reservoir. Many studies have been conducted in the past on reservoir sedimentation, However, very few research has been done specifically on evaluating reservoir capacity using GEE as a tool.

Singh et al. (2018) were the first researchers to utilize the Google Earth Engine (GEE) for estimating the updated capacity of the Gobind Sagar reservoir. They made use of reservoir water elevation data and original reservoir data from 1996/97 for the analysis. The team applied a distinct algorithm to import cloud-free Landsat 8 TOA Reflectance data in GEE, which they later exported to Google Drive. They concluded that assessing reservoir capacity using GEE aids in quick and precise live storage capacity estimation loss due to sedimentation. However, they did not validate the GEE output nor share their findings with other scientists, policymakers, NGOs, field workers, or the general public.

Additionally, Condeca et al. (2022) utilized Google Earth Engine for image selection and automated flooded surface area calculation using water indices. This allowed them to monitor water volume in reservoirs during specific periods by analyzing the relationship between the flooded area and stored volume. They applied this method to four reservoirs and concluded that it has potential as a water management tool in developing nations.

To assess sedimentation in a reservoir, GEE helps to determine the present storage capacity, and the reduction in capacity. Two fundamental tasks must be performed as an input for this method. Firstly, it is essential to choose satellite data from the GEE dataset that meets the analytical requirements. Secondly, the water spread area of the reservoir must be calculated by identifying the most appropriate water index. Utilizing this platform, the water spread area can be determined at various elevations, allowing for the creation of an updated area-elevation-capacity curve. In the context of this study, the availability of satellite data and the effectiveness of the chosen water index are important factors to consider. The capability of the water index to be used and the availability of satellite data to be used were therefore discussed below for the current study.

2.4.1 Satellite Data and Imagery

Earth Engine is a powerful computational service that combines a vast, multi-petabyte data catalog with an efficient and parallel processing system. This data catalog contains a plethora of freely available geospatial information, including images from various satellite and aerial imaging systems, environmental data, weather and climate projections, as well as land cover, topography, and socioeconomic datasets. Updated daily with nearly 6,000 new scenes, the catalog stays current with a typical delay of only 24 hours. The majority of the catalog contains remote sensing images of Earth from various sources.

This platform contains more than 40 years of remote sensing data, including information from Landsat, MODIS, NOAA AVHRR, Sentinel 1, 2, 3, and 5-P, and ALOS satellites (Gorelick et al., 2017). Besides offering a vast collection of raw remote sensing images, users can also access preprocessed, cloud-removed and mosaicked images through the GEE data catalog.

The GEE data catalog contains pre-processed and geo-referenced data from Landsat 4, 5, 7, and 8, which is processed by the US Geological Survey (USGS). This makes it easy to directly use the data. According to Tamiminia et al., (2020), from published research papers utilizing GEE, optical images like those from Landsat and MODIS are the primary data sources used on the platform. Additionally, Landsat-8 is the most widely used mission among all Landsat missions. Thus, from the discussed literatures, utilization of Landsat is beneficial.

2.4.2 Surface water extraction indices

Identifying land cover types and examining changes are some of the primary uses of remote sensing. A fundamental task is distinguishing water bodies from built-up land surfaces. To do this, open water features are outlined using band information extraction techniques. While numerous water extraction algorithms have been created and utilized for remotely sensed images, water indices remain the most popular methods due to their ease of use and reduced computational time compared to other approaches. The most commonly used water indices include the Normalized Difference Water Index (NDWI), Modified NDWI (MNDWI), and Automated Water Extraction Index (AWEI) (Acharya et al., 2018).

The Normalized Difference Water Index (NDWI), introduced by McFeeters (1996), was designed to highlight open water features and improve their visibility in remote-sensing digital images. Similar to the principles used in developing the Normalized Difference Vegetation Index (NDVI), NDWI uses near-infrared radiation and visible green light to emphasize open water features while reducing reflectance from built-up areas. The NDWI is expressed as follows:

$$NDWI = \frac{GREEN - NIR}{GREEN + NIR}$$

In this context, GREEN refers to a band that represents the reflected green light, while NIR represents the reflected near-infrared radiation. The selection of these wavelengths serves three primary objectives: increasing the typical reflectance of water features through the use of green light wavelengths, minimizing the water features' low reflectance of NIR, and benefiting from the high reflectance of NIR exhibited by land-based vegetation and soil features. According to McFeeters (1996), applying the specified equation to process a multispectral satellite image with both a visible green band and an NIR band will result in positive values for water features, while other land features, including soil and terrestrial vegetation, will generate zero or negative values.

Xu (2006) modified the Normalized Difference Water Index (NDWI) to improve its effectiveness in distinguishing between built-up surfaces and water pixels. By analyzing spectral reflectance patterns for three land cover types - water, vegetation, and built-up land - in a sample study area, it was determined that both water and built-up surfaces had higher green light reflectance as opposed to near-infrared light. This indicates that the application of the NDWI produces a positive value for built-up land just as for water. Therefore, by substituting the middle infrared (MIR) band in place of the near-infrared (NIR) band within the NDWI, negative values would be assigned to built-up land areas. This adjustment led to a modified NDWI, offering improved accuracy in differentiating between built-up surfaces and water. Recent literature provides various methods for water extraction using remote sensing imagery, including the use of Landsat imagery and GIS to estimate the hydrologic connectivity of wetlands (Gao et al., 2018), and the use of machine learning approaches and water index-based methods for monitoring land use and land covers (Liu et al., 2020). The modified NDWI (MNDWI) is then expressed as:

$$MNDWI = \frac{Green - MIR}{Green + MIR}$$

The same author, examined and contrasted MNDWI and NDWI approaches, focusing on three primary open water forms: ocean, lake, and river, utilizing Landsat imagery. The findings revealed that MNDWI is more suitable for the enhancement of water with many built-up land areas in the background than the NDWI because it can capably reduce and even eliminate built-up land noise. Hence, it was concluded that by modifying the NDWI technique with a MIR band instead of a NIR band, the enhancement of open water characteristics can be significantly improved.

Despite significant advancements, water classification accuracy still faced major challenges, particularly in areas with diverse land covers like urban roads and shadows from mountains, buildings, and clouds. To address this, Feyisa et al. (2014) developed a new Automated Water Extraction Index (AWEI) that enhances the accuracy of water area classification in the presence of shadows and dark surfaces. The primary goal of AWEI was to optimize the distinction between water and non-water pixels using band differencing, addition, and varying coefficients. As a result, two separate equations were proposed to effectively suppress non-water pixels and achieve more accurate surface water extraction.

$$AWEI_{nsh} = 4 \times (\rho_{band2} - \rho_{band5}) - 0.25 \times \rho_{band4} + 2.75 \times \rho_{band7}$$

$$AWEI_{sh} = \rho_{band1} + 2.5 \times \rho_{band2} - 1.5 \times (\rho_{band4} - \rho_{band5}) - 0.25 \times \rho_{band7}$$

The $AWEI_{nsh}$ index is suitable for situations where shadows are not a significant issue, while the $AWEI_{sh}$ index is specifically designed to remove shadow pixels and improve water extraction accuracy in areas with shadows or other dark surfaces. In the first equation, the difference between band 2 and band 5 is multiplied by four, resulting in large positive values for water pixels and negative values for most non-water pixels. To further differentiate water from other similar surfaces, band 4 and band 7 are subtracted with different weights. As a result, the AWEI is recommended as a superior water index, especially for extracting water data in areas where noise from shadows and built-up surfaces may cause issues.

2.4.2.1 Selecting appropriate water index

The selection of suitable water index is essential for precise detection and monitoring of water resources. Consequently, choosing a suitable water extraction index is a critical aspect of any research. Recognizing this, various researchers have recently compared and assessed different water indices from different parts of the globe to determine the most suitable water index.

Feyisa et al. (2014) Landsat 5 TM images were utilized to evaluate the precision and dependability of AWEI in diverse water bodies at five locations across the world. The effectiveness of AWEI was examined in comparison with the MNDWI and Maximum Likelihood (ML) classification methods. AWEI demonstrated significantly superior accuracy in four out of the five examined locations. Nevertheless, in a region with minimal shadow surfaces, both AWEI and MNDWI yielded comparably precise outcomes. Consequently, the study determined that the application of AWEI can substantially enhance accuracy in areas where shadows and other dark surfaces primarily contribute to classification inaccuracies.

Zhai et al. (2015) evaluated the water detection capabilities of various indices, including NDVI, NDWI, MNDWI, and AWEI, in two distinct locations - an urban site and a rural one. They found that the AWEI and MNDWI indices were more effective in distinguishing water from shadows in urban areas, while the MNDWI emerged as the most appropriate index for water body identification in rural areas. Similarly, Singh et al. (2015) conducted a study to evaluate the effectiveness of the NDWI and MNDWI for detecting water bodies intertwined with vegetation using satellite imagery. They found that MNDWI is a more effective tool than NDWI for detecting water bodies interwoven with vegetation in satellite imagery. Recent literature provides various methods for water extraction using remote sensing imagery, including the use of Landsat imagery and GIS to estimate the hydrologic connectivity of wetlands (Gao et al., 2018), and the use of machine learning approaches and water index-based methods for monitoring land use and land covers (Liu et al., 2020).

Moreover, by using Google Earth Engine (GEE) Condeça et al, (2022), evaluated various water indices, specifically NDWI $_{McFeeters}$, NDWI $_{Gao}$, and MNDWI, in determining the optimal index for image analysis with Landsat imagery at distinct reservoirs. Their findings revealed that, despite its tendency to overestimate water areas, the NDWI $_{Gao}$ was not as effective as the NDWI $_{McFeeters}$ and MNDWI methods in identifying and delineating water-containing pixels. Additionally, the NDWI method's performance weakened in comparison to the MNDWI method which delivered superior results. Upon evaluation and through statistical analyses, the MNDWI index emerged as the top-performing index among the three, offering values more closely approximated measurements, along with impressive correlation coefficients ranging from 0.96 to 0.99.

Similar study by using Google Earth Engine (GEE) Zhang et al., (2017), a multispectral water index was employed to analyze reservoir area from Landsat imagery. This study focused on extracting the area of 200 major reservoirs in Texas, utilizing the Modified Normalized Difference Water Index (MNDWI) for this purpose. The findings validated the effectiveness of MNDWI as a spectral index for water identification and highlighted the spatial heterogeneity of MNDWI thresholds at the regional level. Moreover, Tew et al., (2022), investigated the abilities of three water indices MNDWI, NDWI, and AWEI, for aquaculture pond mapping in Sungai Udang, using GEE. For each water index, the threshold for water pixel extraction was consistently set at 0. The results demonstrated that MNDWI outperformed the other indices, achieving an accuracy of 81.87% and a Kappa coefficient of 0.61.

The research findings clearly demonstrate that water indices effectively delineate open water features with accuracy. Among the three evaluated indices (NDWI, MNDWI, and AWEI), (MNDWI proves to be highly effective in extracting water bodies like reservoirs and lakes from satellite imagery. This is particularly true in areas devoid of urban or built-up land cover, where shadows and other land classes do not hinder water detection.

3 MATERIALS AND METHODS

3.1 Study Area

3.1.1 Koka Reservoir

The Koka Dam was built in 1960 with the goal of generating hydroelectric power, located on the Awash River in central Ethiopia (8°26'N, 39°2'E). The dam was designed with an original storage capacity of 1,650 million cubic meters at a full supply level of 1,590.7 meters above sea level or 110.3 meters reduced level. The Awash River originates in the highlands and is known for its high peak flash floods, which carry a large amount of sediment. Consequently, it is expected that the water storage capacity of the dam will face significant challenges from siltation.

The Reservoir is situated 90 km south of Addis Ababa at an elevation of 1600 m. It has a surface area of 200 km^2. Ethiopian Electric Power (EEP) operates the dam with the Ethiopian Ministry of Water and Energy (MoWE), providing guidance and oversight. The dam was mainly constructed for hydropower production, with an installed capacity of 43.2 MW from its three turbines, contributing to 5% of Ethiopia's overall grid-connected power generation capacity. However, newer and larger reservoirs overshadow the energy contribution of Koka (Mamo, 2002). The Koka Dam, built with concrete, has a length of 458 m and a maximum height of 47 m. It utilizes a head of 32-42 meters, with 132 kV transmission lines. Table 3-1 shows a general description of the dam.

Table 3-1 General Description of The Koka Dam

Features	Koka reservoir
Construction Year	1960
Installed capacity	43.2 MW
Gross storage capacity	1650Mm^3
Surface area	200 km^2
Dam Hight	47 m
Type of dam	Concrete gravity dam

3.1.2 Gefersa I/II Dam

The Gefersa I/II Dam located approximately 18 km northwest of Addis Ababa city along the Addis-Ambo Road. It is situated in the Oromia National Regional State within the Sheger City Administration. The project area is situated in the upper part of the Akaki sub-basin (part of the

Awash River basin), with coordinates of 38^{0}34’30”-38^{o}40’50” E, and an elevation range of 2587.0 to 2957.0 m.a.s.l. The Geffersa I/II dam was built in 1943 (and was modified in 1955). The Gefersa I/II dam underwent successive modifications, in 1943 (originally built as a 10 m high masonry dam), in 1955, the dam was raised by 6 m, and finally, in 2009, a major rehabilitation work (renovation of the dam body and hydraulic works) (ECDSWC, 2017).

The dam was primarily built with homogeneous clay soil as the main construction material. Fine gravel was used to create a 45m long and 0.8m thick phreatic line that runs through the foundation of the dam. The embankment's total bed width is 149.35m, while the top width is 5m. The dam stands approximately 19m above the riverbed. The slopes on the upstream and downstream sides of the embankments are 1V:2.58H and 1V:2.27H respectively. The reservoir is situated in a 10-kilometer-wide shallow basin, located between the Wechacha and Intoto mountains. Under the existing reservoir management, the Gefersa I/II system provides water to the Gefersa treatment plant (BirdLife International, 2023). Table 3-2 shows a general description of the dam.

Table 3-2 General Description of The Gefersa I/II Dam

Feature	**Gefera I/II dam reservoir**
Construction Year	1943
Purpose	Water supply
Dam Hight	19m
Type of dam	Homogeneous
Full supply level	2587.1 m.a.s. l
upstream Catchment area	56 km^2
U/S and D/S slope	1V:2.58H and 1V:2.27H
Gross storage capacity	11.82 MCM

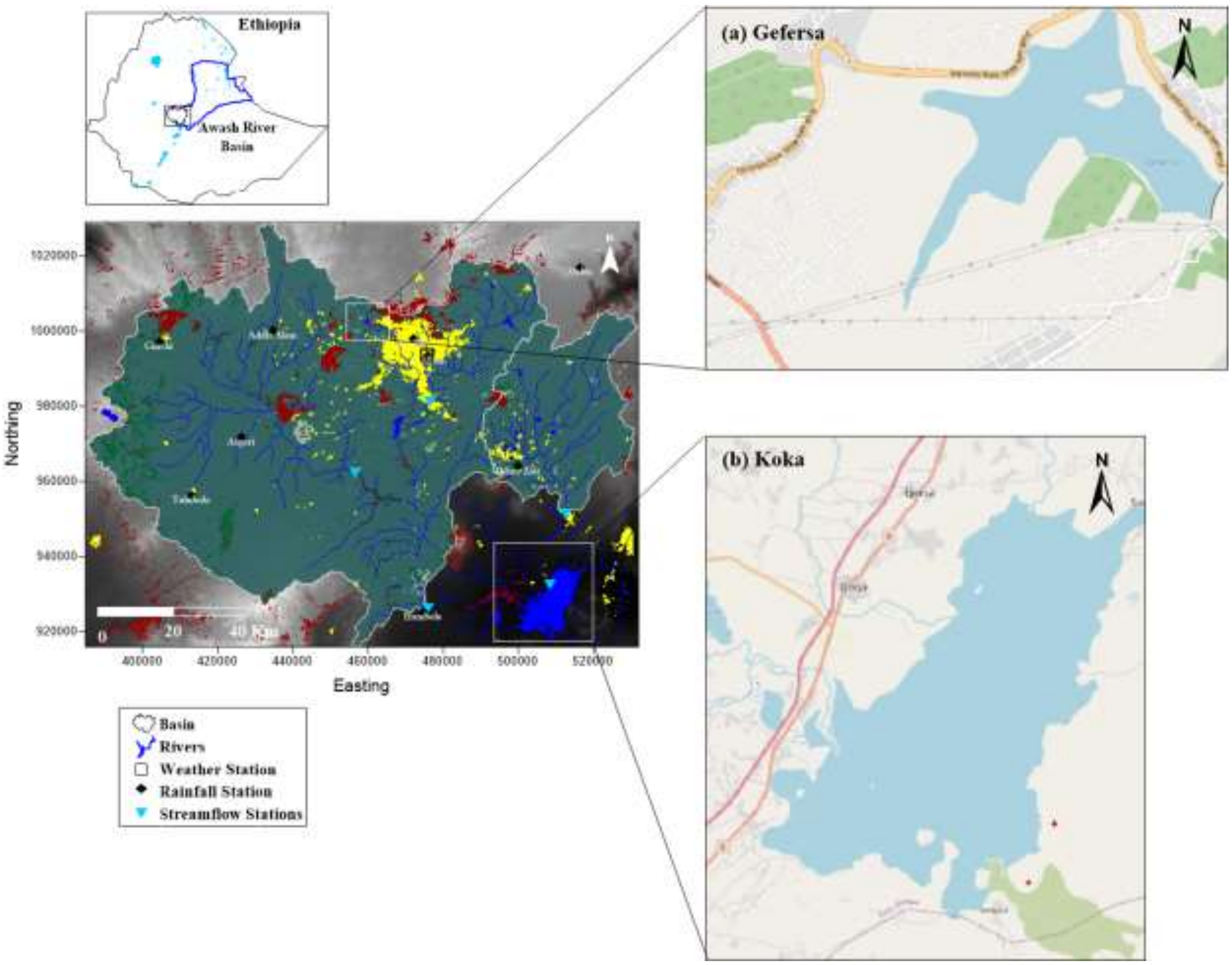

Figure 3-1 Location map of the study area

3.2 Data and Tools Used

3.2.1 The Google Earth Engine Platform

Google Earth Engine serves as a cloud-based platform aimed at facilitating large-scale geospatial analysis by utilizing Google's vast computational power to tackle various significant societal challenges (Gorelick et al., 2017). By offering a multi-petabyte repository of satellite images and geospatial data, coupled with global-scale analytical tools, this platform empowers scholars, investigators, and developers to detect changes, plot trends, and quantify variations on the Earth's surface(Singh et al., 2018). Furthermore, the platform is openly available and easy to use, providing a conducive environment for the development of algorithms. Therefore, it has empowered scientists, researchers, and communities to analyze data, generate trend maps, and identify resources on the Earth's surface (Kumar & Mutanga, 2018).

The GEE platform offers a free, open-access API for Python and JavaScript languages, incorporating cloud computing and ready-to-use processing functions (Gorelick et al., 2017). On the one hand, it can be accessed through a web-based IDE using the JavaScript API, allowing users to visualize images, results, tables, and charts for easy exportation. On the other hand, the Python API provides similar methods for making requests and accessing the catalog, but without the visualization features of the web-based IDE. Therefore, in this study, the JavaScript API was chosen to obtain and treat Landsat satellite images.

3.2.2 Reservoir Data

The original reservoir information before the impoundment was utilized, along with recent bathymetric survey data. In a 1999 study of flood management of the Koka Reservoir and power planning during low water years, the Hydrology Department of the Ministry of Water and Energy carried out the Koka Reservoir hydrographic survey. Thus, 1999 bathymetric survey data were acquired from the Ministry of Water and Energy. Similarly, the bathymetry survey of the Gefersa I/II reservoir in 2017 was obtained from Gefersa intake rehabilitation and bathymetric survey work project, conducted by Ethiopian Construction Design and Supervision Works Corporation (ECDSW). These datasets were used for comparison with the current revised storage capacity and to consider the original capacity of the reservoir for calculating the present sediment deposition.

3.2.3 Field data

To predict sedimentation from the reservoir, it is necessary to have records of annual maximum and minimum observed variation in water levels covering most of the live storage zone, that is, from MDDL to FRL. Thus, daily observed water level (Elevation) data with Elevation data corresponding to the satellite image for the reservoirs was required. For the Koka reservoir, the records of observed reservoir water surface elevation data were obtained from the Koka dam authority from the years 1959 to 2022. Similarly, the records of the observed reservoir water surface elevation data of the Gefersa I/II reservoir were obtained from the Addis Ababa water supply and sewerage authority (AAWSA).

3.2.4 Satellite data

To carry out an assessment of the reservoir sedimentation, the availability of cloud-free satellite images is important. The Google Earth Engine (GEE) data catalog offers optical satellite imagery from 1972 until now, allowing researchers to perform earth-monitoring investigations. Google Earth Engine platform provided Landsat 8 Collection 2 Tier 1 calibrated top-of-atmosphere (TOA) reflectance with a spatial resolution of 30m x 30m. Landsat 8 images are freely available to the public for studies related to the Earth's system. Landsat 8 Operational Land Imager (OLI)/ Thermal Infrared Sensor (TIRS) image collection for the period of analysis 2021-2022 was used in this study.

For the case of the Koka Reservoir, the most recent bathymetric survey available was conducted in 1999. Consequently, utilizing these data for validation purposes may result in significant differences when compared to the present findings. To address this issue, sedimentation study of the Koka Dam in 1999 using GEE was undertaken, employing the Landsat 5 Enhanced Thematic Mapper (ETM) for the period of analysis 1998-1999. This approach will enable the validation of the methodology, while bringing it into line with the existing bathymetric survey results.

3.3 Method

The study used the Google Earth engine platform to quantify sediment accumulation in the selected reservoirs. The main concept of the study is to use Landsat images on the GEE platform to analyze the water spread area of a reservoir at various water levels between MDDL (Minimum Drawdown Level) and FRL (Full Reservoir Level). The sedimentation process causes a continuous decrease in the water spread area of the reservoir at different heights. Hence, by employing the trapezoidal formula and using the water spread area as an input, the reservoir's volume can be calculated. By summing up these values, the total capacity can be determined, enabling to develop area-elevation-capacity curves. Any shift in the capacity curve will indicate the loss of reservoir capacity.

3.3.1 Image importing and pre-processing

3.3.1.1 Importing Landsat image

In this study, data from the Landsat 8 Operational Land Imager (OLI) and Landsat 5 Thematic Mapper (TM) were obtained from the GEE data catalog using separate algorithms. The USGS sorts this data into three categories for each satellite: Tier 1 (high-quality geometric and radiometric data), Tier 2 (data not meeting Tier 1 standards), and Real-Time (data not yet evaluated). The highest quality data is placed in Tier 1 and is considered suitable for time-series analysis. Tier 1 includes Level-1 Precision Terrain (L1-TP) processed data that have well-characterized radiometry and inter-calibration across various Landsat sensors (USGS, 2014). All Tier 1 Landsat data can be considered consistent and inter-calibrated (regardless of the sensor) across full collection (USGS, 2014). Therefore, for both reservoirs Landsat 8 OLI and Landsat 5 TM Tier 1 calibrated top-of-atmosphere (TOA) reflectance scenes were used. All of these images are available on the GEE platform and are free to use. Also, an Image visualization variable was created $trueColor432Vis$ which is used to transform numbers into RGB colors. Figure 3-2 and Figure 3-3 below shows the code used to import Landsat 8 OLI and Landsat 5 TM images and their visualization parameters.

Table 3-3 Code used to import Landsat 8 OLI

```
// Import Landsat 8 OLI image
var dataset = ee.ImageCollection("LANDSAT/LC08/C02/T1_TOA");
//Selecting RGB band from the imported image
var trueColor432 = dataset.select(['B4', 'B3', 'B2']);
// Visualization parameter
var trueColor432Vis = {
        min: 0.0,
        max: 0.4,
};
```

Table 3-4 Code used to Import Landsat 5 TM

```
// Import Landsat 5 TM image
var dataset = ee.ImageCollection("LANDSAT/LT05/C02/T1_TOA");
//Selecting RGB band from the imported image
var trueColor321 = dataset.select(['B3', 'B2', 'B1']);
var trueColor321Vis = {
     min: 0.0,
     max: 0.4,
     gamma: 1.2,
```

```
};
```

3.3.1.2 Identifying the area of interest

Due to the vast size of each complete scene and the area of interest was only the reservoir water spread area, it is essential to separate this area from the entire scene in all images. To do so, the JRC Global Surface Water Dataset (GSWD) from the GEE data catalog was imported to visualize the maximum water extent of the reservoirs. This is to incorporate the whole area of the reservoirs for the computation.

The global Surface Water Dataset (GSWD) is a single image of the Spatiotemporal distribution of surface water with 7 bands (Pekel et al. 2016). The max_extent band in GSWD indicates if a pixel ever had water or not, with 0 meaning no water was present in any month, and 1 signifying the pixel had water for at least one month. Therefore, based on this information a polygon was drawn as a study area for both reservoirs as shown in the Figure 3-5. This was done in GEE by using a polygon tool and renamed as $reservoir$. Figure 3-4 shows the code used to identify the study area using GSWD dataset.

Table 3-5 Code used to identify the study area using GSWD dataset

```
var dataset = ee.Image('JRC/GSW1_3/GlobalSurfaceWater');
var max_extent= {
  bands: ['max_extent'],
  min: 0.0,
  max: 1.0,
  palette: ['ffffff', 'ffbbbb', '0000ff']
};
Map.centerObject(reservoir, 12);
var clip = dataset.clip(reservoir);
Map.addLayer(clip.selfMask(), max_extent, 'max_extent');
```

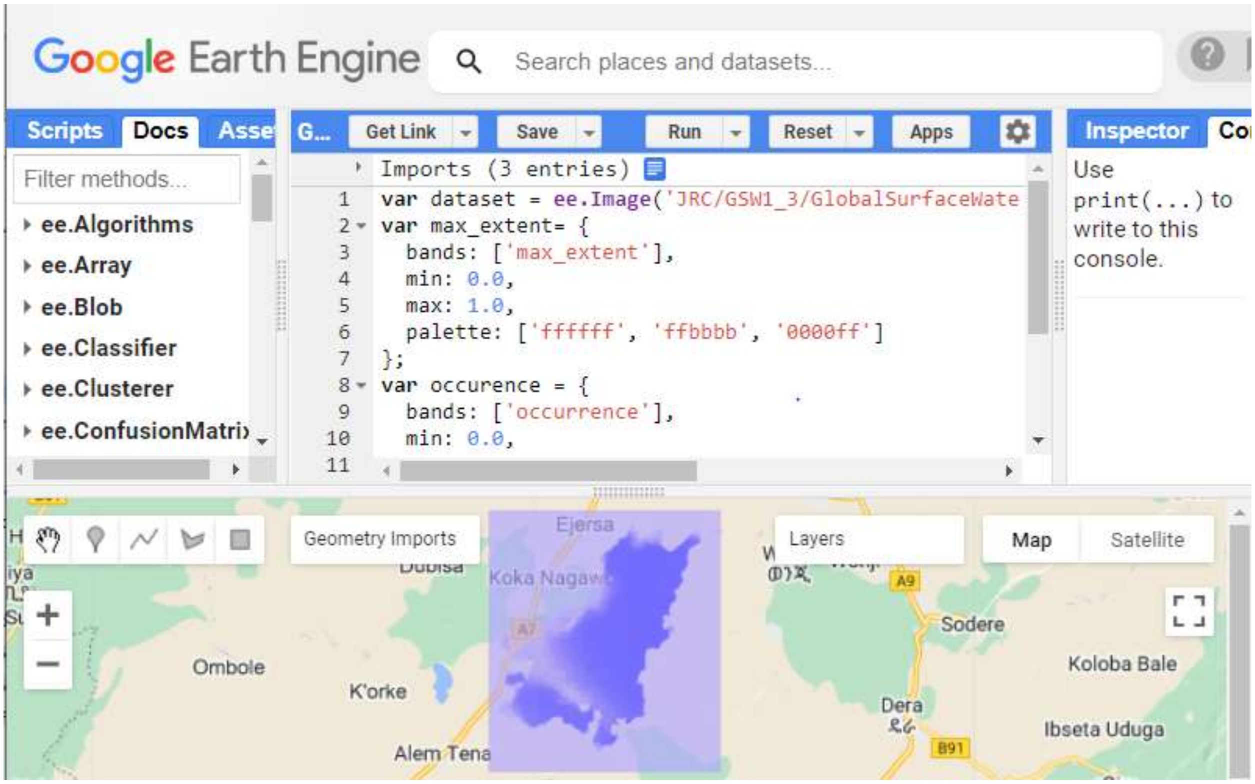

Figure 3-2 Selection of Study Area Using the Polygon Tool

3.3.1.3 Filtering image collections

To calculate the water spread area in each image and generate a map of surface variation of the reservoir, it is essential to obtain high-quality images. Thus, carrying out automatic preprocessing is crucial to ensure that the images collected initially meet the required quality, enabling the acquisition of a suitable image set for the next step. Therefore, each image underwent pre-processing and visualization to ensure that each image utilized covered the full reservoir. In addition, the images might be covered by clouds and shadows, and a filter must be applied. Thus, three different types of filters were used in the current investigation under $ee.Filter$ function in GEE. These are Filter by metadata, Filter by date, and Filter by location. To select images in a particular date range and to select the subset of images with a bounding study area $ee.Filter.date()$ and $ee.Filter.bounds()$ were used, respectively. Following that, images with less than 10% cloud cover were carefully chosen using an $ee.Filter.lt$ (‘$CLOUD\_COVER$’, 10). Therefore, the code below was used to filter at a specific date and filter images with cloud cover less than 10% using “$CLOUD\_COVER$” attribute present as a property of the images. Figure 3-6 shows the code used to filter Landsat imagery.

Table 3-6 Code used to filter Landsat imagery

```
// Filter image by metadata, date, and boundary
var jun_01_2022 = dataset.filter(ee.Filter.date('2022-06-01', '2022-06-02'))
                          .filter(ee.Filter.bounds(reservoir))
                          .filter(ee.Filter.lt('CLOUD_COVER', 10))
                          . map(maskL8sr);
```

3.3.1.4 Masking

The Top of Atmosphere products from the Landsat 5 and 8 satellites have been processed with radiometric calibration, and atmospheric and geometric correction as mentioned earlier. The extra necessary processing for the images includes masking of the low-quality observations, i.e., the pixels contaminated by cloud, cloud shadow, and terrain shadow. Detecting clouds, cloud shadows, and snow in satellite imagery is crucial, as they must be accurately screened prior to conducting any remote sensing tasks (Zhe et al., 2015). Previously, in the filtering process for the problem related to the presence of clouds, Images with cloud cover greater than 10% were removed using a filter on the "$CLOUD\_COVER$" attribute. However, this does not guarantee the elimination of pixels containing clouds over the reservoir region, and it may exclude images where the clouds do not obstruct the reservoir area (Condeça et al., 2022).

Therefore, it was recommended to mask the clouds and cloud shadow using the "*QA _PIXEL*" band of Landsat TOA images by encoding the correct cloud mask functions (GEE, 2020). The "*QA _PIXEL*" band in Landsat 8 OLI is a part of the quality assessment dataset provided by USGS, that encodes various quality attributes such as cloud cover, cloud shadow, cirrus confidence, and snow/ice (USGS, 2020). Therefore, the "*QA _PIXEL*" bands were imported and developed a single function maskL85 allowing to mask of the pixels with clouds and cloud shadows for Landsat 8 and 5 on top of the reservoir area. Thus, this function was applied together with the filtering process. Figure 3-7 shows the function developed for cloud and cloud shadow masking.

Table 3-7 Function for cloud and cloud shadow masking

```
// This function masks clouds and cloud shadows,
var maskL85 = function(image) {
  var cloudShadowBitMask = ee.Number(2).pow(3).int();
  var cloudsBitMask = ee.Number(2).pow(5).int();
  var qa = image.select('QA_PIXEL');
  var mask = qa.bitwiseAnd(cloudShadowBitMask).eq(0)
      .and(qa.bitwiseAnd(cloudsBitMask).eq(0))
      .and(qa.bitwiseAnd(ee.Number(2).pow(0).int()).not());
  return image.updateMask(mask);
};
```

3.3.1.5 Composite and Clipping

After the filtering and cloud masking all the available images were composited and clipped. Compositing is the process of merging spatially overlapping images into a single image using an aggregation function. Using GEE, it is possible to create a composite image by applying the $.median()$ function. Following the formation of a composite image, it is preferable to clip the images to the region of interest. This clipping process eliminates irrelevant sections of a sizable image, conserving computational resources and time. Therefore, by using $.clip(reservoir)$ function unnecessary portion of an image was removed.

Table 3-8 Code used to clip and composite

```
// creation of a single image
var composite_image = filtered_image.median();
// Clipping image
var clip_image = composite_image.clip(reservoir);
```

After applying the above image pre-processing codes, the output image was then visually inspected carefully and selected the most appropriate list of images based on the water level of the reservoir. For both study areas, eight cloud-free images were selected as shown in Table 3-4 and Table 3-5.

In addition, for the analysis in 1999, eight cloud-free images were obtained for the Koka reservoir as shown in Table 3-3.

Table 3-9 Koka reservoir 1999

date of satellite pass	Cloud Cover	Satellite and sensor	Elevation
Jun /18/1999	<10%	Landsat 5 TM	1583.7
Jul/17/1998	<10%	Landsat 5 TM	1584.11
Mar/30/1999	<10%	Landsat 5 TM	1586.08
Feb/26/1999	<10%	Landsat 5 TM	1586.98
Feb/10/1999	<10%	Landsat 5 TM	1587.42
Dec/24/1998	<10%	Landsat 5 TM	1588.66
Nov/9/1999	<10%	Landsat 5 TM	1589.42
Nov/6/1998	<10%	Landsat 5 TM	1590.6

Table 3-10 Koka Reservoir 2021/2022

Date of satellite pass	Cloud Cover	Satellite and sensor	Elevation
Jun/01/2022	<10%	Landsat 8 OLI	1583.54
May/29/2021	<10%	Landsat 8 OLI	1585.23
May/13/2021	<10%	Landsat 8 OLI	1585.61
Mar/26/2021	<10%	Landsat 8 OLI	1586.63
Feb/25/2022	<10%	Landsat 8 OLI	1587.58
Dec/26/2022	<10%	Landsat 8 OLI	1588.94
Nov/21/2021	<10%	Landsat 8 OLI	1589.99
Sep/21/2022	<10%	Landsat 8 OLI	1590.7

Table 3-11 Gefersa Reservoir I/II 2021/2022

Date of satellite pass	Cloud Cover	Satellite and sensor	Elevation
Jun_24_2022	<10%	Landsat 8 OLI	2580.01
May_16_2022	<10%	Landsat 8 OLI	2581.27
May_29_2021	<10%	Landsat 8 OLI	2582.72
Mar_13_2022	<10%	Landsat 8 OLI	2583.41
Feb_09_2022	<10%	Landsat 8 OLI	2584.47
Jan_21_2021	<10%	Landsat 8 OLI	2585.67
Nov_21_2021	<10%	Landsat 8 OLI	2586.61
Nov_05_2021	<10%	Landsat 8 OLI	2587.11

3.3.1.6 Calculating water index

A decrease in the water spread area of specific water levels can represent the reduced capacity of a reservoir. One of the methods for mapping water spread area is through water indices(Chen et al., 2023). The water index plays a critical role to detect and delineate surface water by emphasizing the spectral characteristics of water features using band math (Tew et al., 2022). For the present study the most widely used water index, Modified Normalized Difference Water Index (MNDWI) was used for extracting water pixels. As discussed in the previous chapter, MNDWI is introduced by Xu (2006), it’s a powerful index for extracting water bodies such as reservoirs and lakes from satellite images, especially in areas with no urban or built-up land cover, where shadows and other land classes do not interfere with the water detection. The modified Normalized Difference Water Index (MNDWI) is expressed as:

$$MNDWI = \frac{Green-MIR}{Green+MIR}$$

Where GREEN is a band that represents reflected green light and MIR represents middle infrared radiation. Using GEE, it is possible to calculate the water index using $ee.Image.normalizedDifferene$ helper function. This function computes the normalized difference between two bands. In GEE the normalized difference is computed as (first band− second band) / (first band+ second band). Thus, the MNDWI computation is performed on Landsat 5 imagery using bands 2 (green) and 5 (SWIR), and on Landsat 8 imagery using bands 3 (green) and 6 (SWIR).

The modified normalized difference water index (MNDWI) values are used to distinguish water pixels from non-water pixels by implementing a threshold. These values range from -1 to 1, with 0 serving as the threshold. Water pixels exhibit positive values because they have greater reflectance in the green band compared to the SWIR band, whereas non-water pixels have negative values due to their lower reflectance in the green band relative to the SWIR band (Xu, 2006). For the village site, which is covered by simple features, the threshold 0 is frequently selected in the water extraction processing (Zhai et al., 2015). In addition, several studies have reported that a standard threshold of 0 for MNDWI is effective for extracting reservoirs and lakes from satellite images(Condeça et al., 2022; Tew et al., 2022). Based on that, for the present study, a standard threshold of 0 was used for extracting reservoirs. The function in Figure 3-9 was used to calculate both the spectral index and to map the flooded area of the reservoirs for each image.

Table 3-12 Function to calculate both the spectral index and to map the flooded area

```
// a function to calculate NDWI and MNDWI
var calculate_ndwi = function (image, name) {
  //Add the NDWI band to the image
  var ndwi = image.normalizedDifference(['B3','B6']).rename(['ndwi']);
  // Determining the threshold value
  var Threshold = 0
 //Extract water pixels greater than the threshold value
 var water_pixels = ndwi.gt (Threshold)
  image = image.addBands(ndwi)
  Map.centerObject(reservoir, 10)
  Map.addLayer(water_pixels, visparam, name)
```

After applying the above function, the MNDWI map of all images was displayed in the platform and exported to the drive. However, discontinuous water pixels were observed in the vicinity of the reservoir. Thus, these isolated water pixels surrounding the water spread area were removed. Similarly, water pixels downstream of the reservoir were not a part of the reservoir area, hence were removed.

3.3.2 Calculation of Water Spread Area

After identifying the water pixels for the area of interest in both reservoirs, the water spread area for each cloud-free dates of pass for each reservoir were calculated using the following equation (Foteh et al. 2018).

$$\text{Water spread area} = \frac{\text{No. of water pixels} * \text{pixel area}}{1{,}000{,}000}$$

The process of calculating the area of images in GEE involves utilizing the $ee.Image.pixelArea()$ function. The $ee.Image.pixelArea()$ function generates an image in which the value of each pixel represents its area. To obtain the total area, the pixel area image is multiplied with the MNDWI image, and the resulting values are summed using the $reduceRegion(\ )$ function. The $ee.Image.pixelArea()$ function employs a modified equal-area projection to determine the area, ensuring that the final result is expressed in square meters, irrespective of the input image's projection. To convert into a square kilometer, the area of water is added to the band and divided by $1*10^6$. The code in Figure 3-10 was used to calculate the water spread area of the reservoirs.

Table 3-13 Code used to calculate the water spread area of the reservoirs

```
// a function to calculate the area
  var area_img = water_pixels.multiply(ee.Image.pixel area())
  var reduce = area_img.reduceRegion({
    reducer: ee.Reducer.sum(),
    geometry: reservoir ,
    scale: 10,
    maxPixels: 1e10
  })
  // adding area of water as a band
  image = image.addBands(area_img);
  // convert to square kilometers
  var SqKm = ee.Number(reduce.get('ndwi')).divide(1e6).round();
```

```
  print ('area of water pixels at ',  name ,  SqKm);
};
```

3.3.3 MNDWI Automated Function

The above code used for calculating the MNDWI, thresholding, mapping the MNDWI image, and calculating the area of water pixels was incorporated into a single function to minimize time. This efficient approach significantly reduces the time, as it does not need to repeat the code for each image individually. Moreover, this consolidated function has designed with ease of use in mind for future studies, ensuring that it is both accessible and concise for other users. To further simplify the process, the function only requires the input of an image and its corresponding name, which serves as a means of identification throughout the analysis.

Following the importing and automated pre-processing of the image, it is directly fed into the MNDWI function without necessitating any additional steps. This seamless integration is simplified by the code provided below.

Table 3-14 Code to call MNDWI function

```
var Calculate_MNDWI= MNDWI_function (image, 'name_of_image')
```

It is crucial to note that automating these processes not only saves time for working with multiple images but also reduces the likelihood of errors introduced by manual repetition. Furthermore, by designing the function to be user-friendly, it promotes collaboration and utilization by others in the field who may have varying levels of programming expertise. Overall, this integrated approach significantly enhances the efficiency, accuracy, and accessibility of the MNDWI algorithm and its subsequent analysis. Therefore, using the above function gives the MNDWI map of the reservoirs from MDDL to FSL of the reservoirs.

3.3.4 Computation of Reservoir Capacity

To calculate the capacity of a reservoir, it is essential to understand the relationship between the water area and the stored volume in the reservoir. The reservoir's capacity between two consecutive elevation levels can be determined using the trapezoidal formula, as shown below (Foteh et al., 2018)

$$V = \frac{H}{3}\{ A1 + A2 + \sqrt{A1 * A2}\}$$

Where H is the difference between RLs or altitude (height) interval; A1 and A2 are water spread areas at RL (1) and RL (2). The volume of the reservoir below the minimum draws down level (MDDL) is assumed to be the same before and after sedimentation. This is because remote sensing-based methodology only calculates the sedimentation rate within the zone of fluctuation of reservoir water level. From the original elevation-area curve, the original areas at the MDDL were obtained by linear interpolation.

The volume between each consecutive level above the lowest observed level were added to determine the total capacity of the reservoir. These cumulative volumes were then compared to the design volumes at the same levels to compute reduced volume. Therefore, the reduced volume is the loss of capacity caused by sedimentation.

3.3.5 Reservoir Area-elevation-capacity Curve

Storage variations or reservoir storage cannot be measured directly. Instead, these can be deduced from estimations of elevation and area. Area-elevation-capacity curves are commonly used to represent a reservoir's storage capacity (Gao, 2015). While this method is simple, it can only be applied to reservoirs with accessible storage information.

The revised reservoir Area-Elevation- Capacity curves for storage capacity can be generated using the calculated Area and Volume combined with the corresponding Elevation data. In this study, the revised area-elevation-capacity curves for Koka and Gefersa reservoirs were created and then compared to the original Area-elevation-capacity curves of these reservoirs. In addition, the area-elevation-capacity curve for the 1999 Koka reservoir survey was also developed to validate the methodology. However, for the case of the Gefersa reservoir, the bathymetry survey of 2017 was directly used for validating the method.

3.4 P-test and T-test

For the present study P-test and T-test statistical tests ware used to determine whether there is a significant difference between the means of the bathymetry survey result and GEE result. The P-value determines whether the hypothesis test results are statistically significant. It gauges how consistent the statistics are with the null hypothesis. If the P-value is small enough, it is possible to conclude that the sample is so incompatible with the null hypothesis that the null can be rejected(Frost, 2017).

The T-test is an inferential statistic used to determine if there is a significant difference between the means of two results and how they are related. T-tests are used when the data sets follow a normal distribution and have unknown variances. The t-test is a test used for hypothesis testing in statistics and uses the t-statistic, the t-distribution values, and the degrees of freedom to determine statistical significance(Frost, 2017).

3.5 Methodology Flow Chart

The complete code of the study component developed in JavaScript is available from https://code.earthengine.google.com/?scriptPath=users%2Fsaminegu6%2FSamuel9029%3AComplete%20Methodology%2FReservoir%20Sedimentation%20Assessment%20

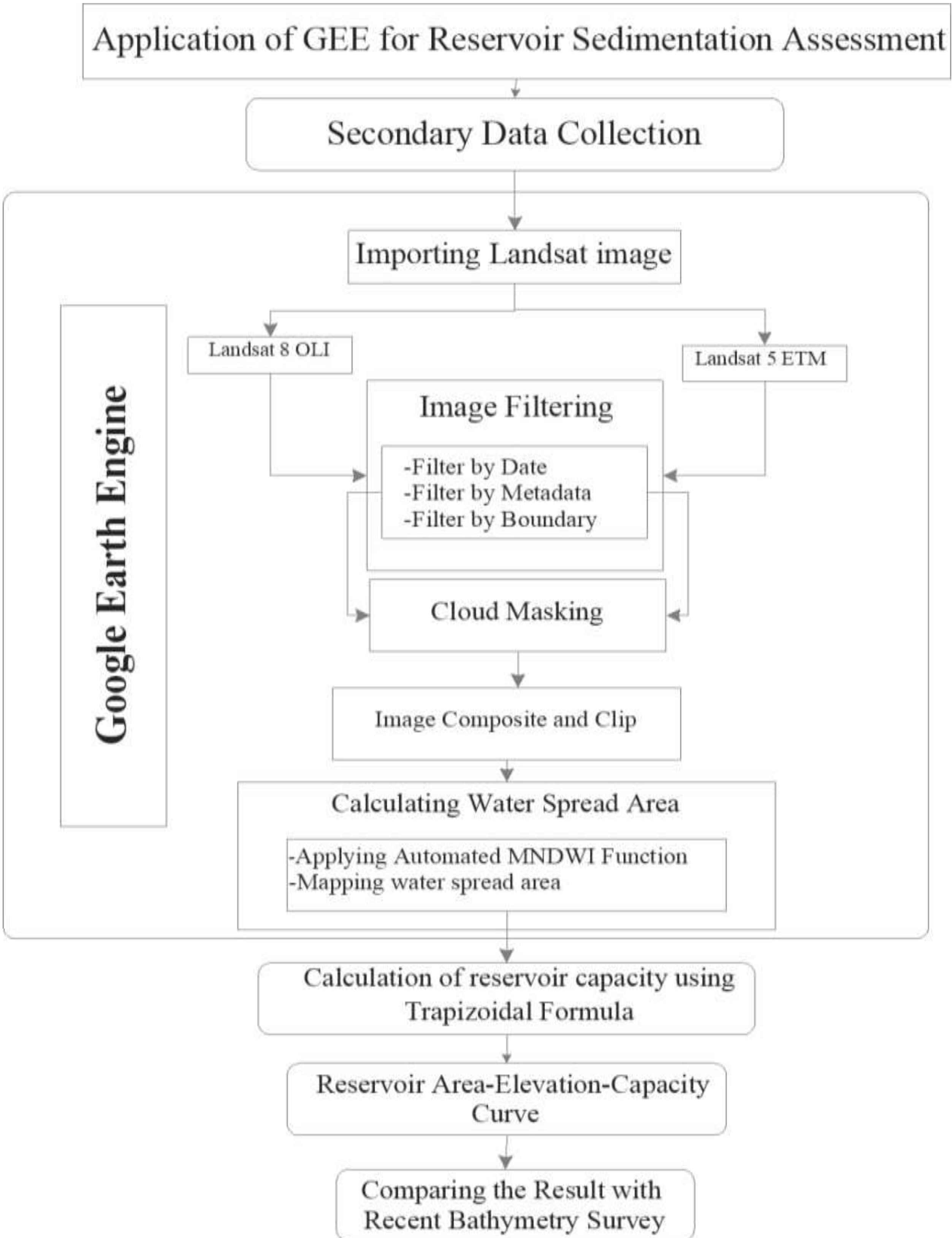

Figure 3-3 Methodology Flow Chart

4 RESULTS AND DISCUSSION

4.1 Estimated water spread area and volume of the reservoirs

In this study, the approach involves processing satellite imagery, calculating the water spread area, and determining reservoir capacity at different elevations. The modified normalized water index (MNDWI) was employed to determine the reservoir's water coverage area. The MNDWI function was used to create a MNDWI map of the reservoirs from the minimum drawdown level (MDDL) to their full supply level (FSL). Figure 4-1, Figure 4-2, and Figure 4-3 shows the MNDWI map of Koka (1999), Koka (2022), and Gefersa I/II reservoir at different Elevations.

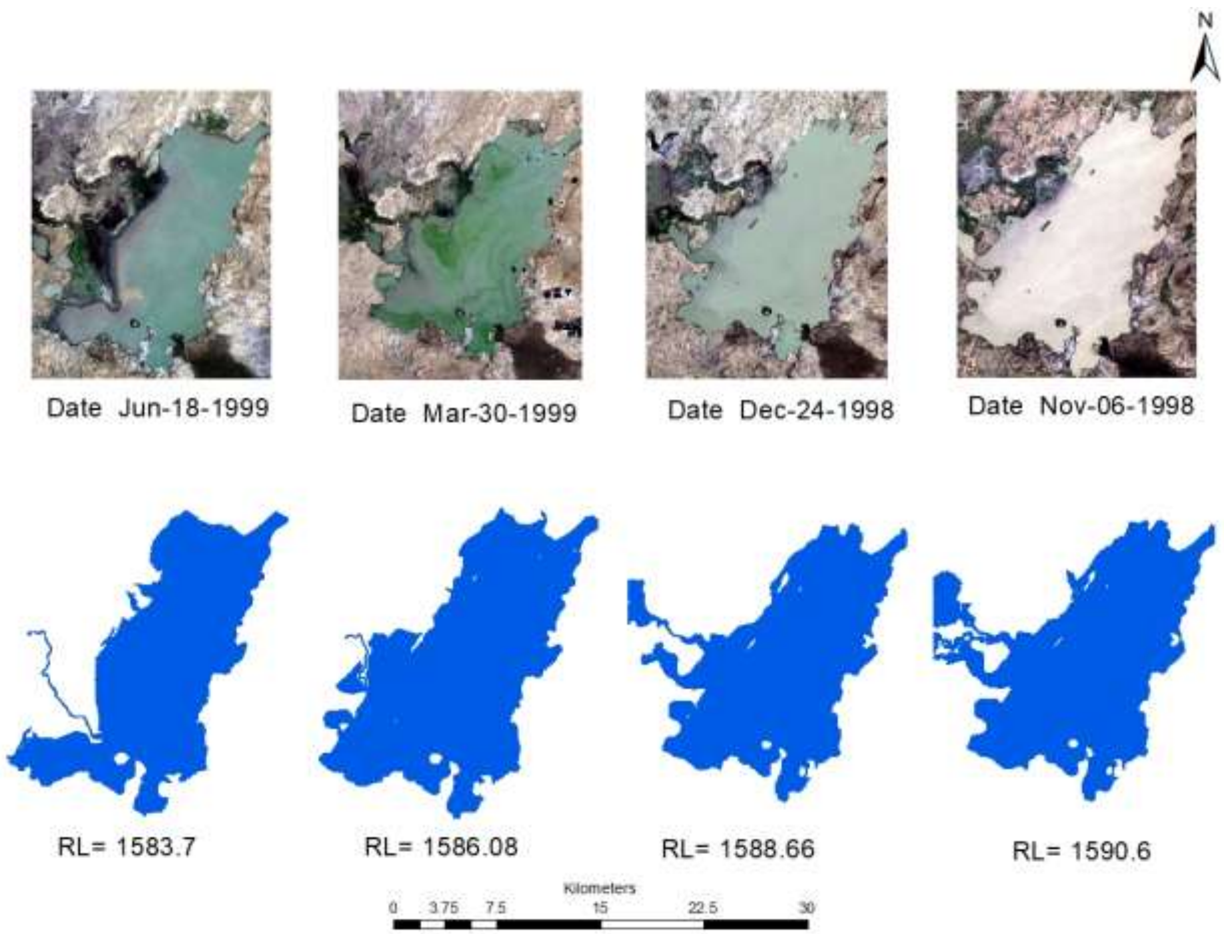

Figure 4-1Water spread area of koka reservoir for the year 1998/1999

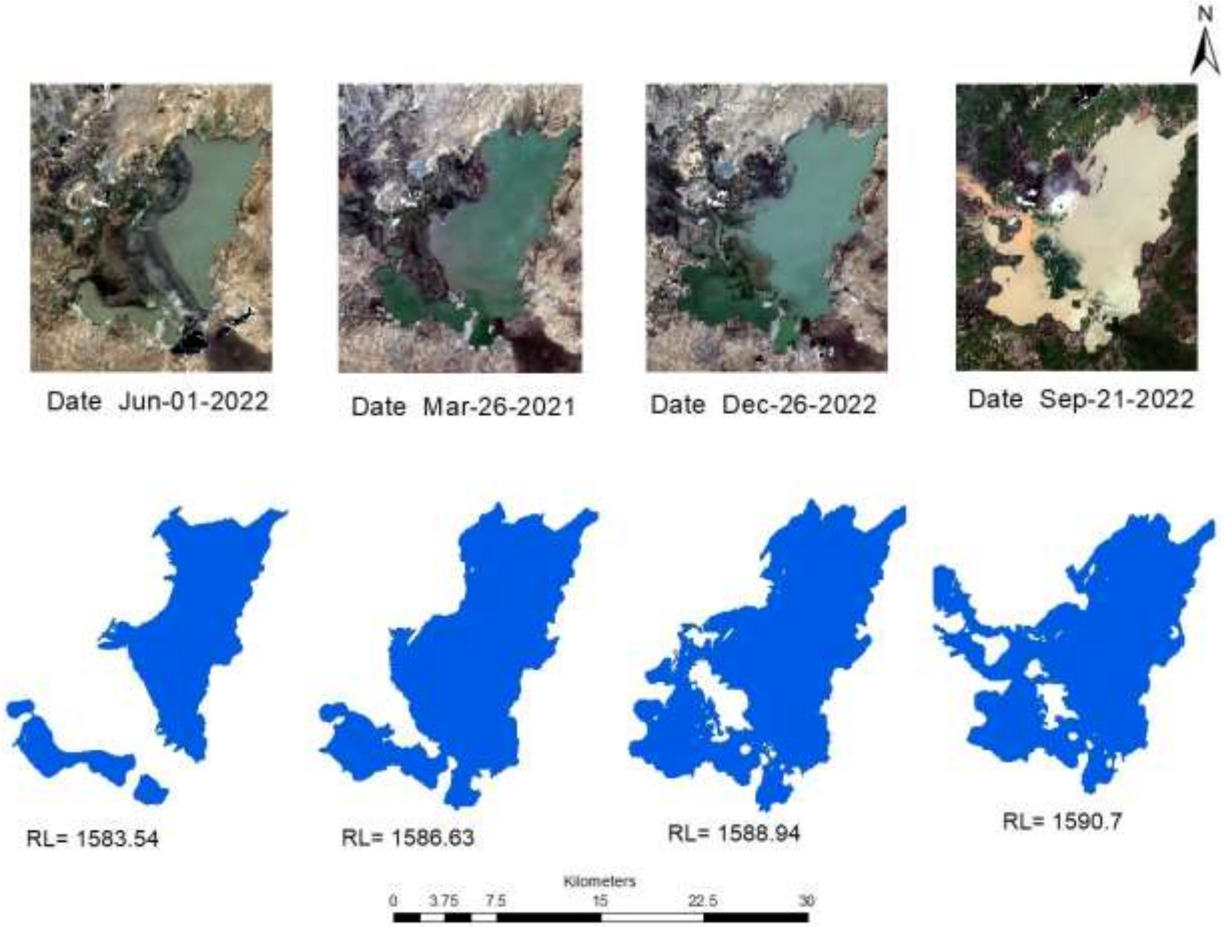

Figure 4-2Water spread area of Koka reservoir for the year 2021/2022

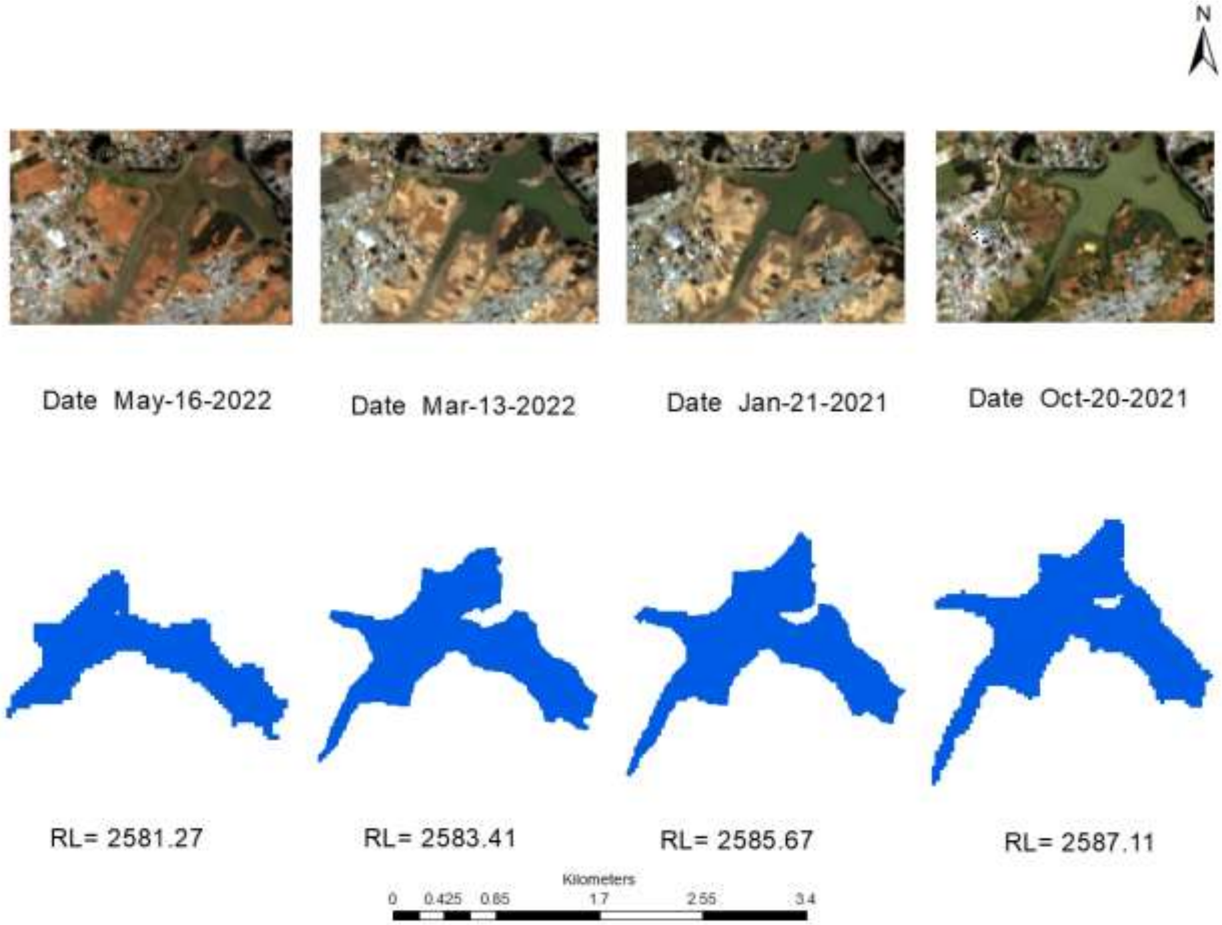

Figure 4-3Water spread area of Gefersa I/II reservoir for the year 2021/2022

Therefore, trapezoidal formula was utilized to calculate the volume between two consecutive reservoir elevations. Afterward, to evaluate the capabilities of Google Earth Engine (GEE) in assessing reservoir sedimentation, a comparison was made with recent bathymetry survey results. This method enables to determine if GEE proves to be a suitable tool for reservoir sedimentation assessment. For the present study, a total of 3 analyses were undertaken.

4.1.1 Reservoir sedimentation of Koka reservoir for the year 1998/1999

The assessment of reservoir sedimentation of the Koka reservoir in 1998/1999 was analyzed. This is due to the constraint of up-to-date bathymetry surveys on the Koka reservoir for comparison. The most recent bathymetric survey available is conducted in 1999. Thus, the 1999 bathymetry survey was employed to compare the outcomes with GEE, by conducting a sedimentation assessment of the Koka Dam for the year 1999. This approach will enable validation of the methodology while bringing into line the results from GEE with the existing bathymetric survey results.

In the analysis, it was assumed that the cumulative revised capacity of the reservoir at its lowest observed level (1583.7m.a.s.l) was equal to the 1999 bathymetry data's cumulative capacity (150.917 Mm^3). The storage capacities above the MDDL to the FSL were added up to estimate the cumulative revised capacities. Table 4-1 shows the estimated cumulative volume based on different date of satellite pass, which is utilized for determining sediment accumulation in the reservoir.

Table 4-1 Area and cumulative volume obtained from koka reservoir using GEE for the year 1998/1999

Date of satellite pass	Elevation	Area (Km^2)	Volume (Mm^3)	Cumm. Volume (Mm^3)
Jun /18/1999	1583.7	121	150.917	150.917
Jul/17/1998	1584.11	136	52.655	203.572
Mar/30/1999	1586.08	156	289.395	492.967
Feb/26/1999	1586.98	163	143.538	636.505
Feb/10/1999	1587.42	167	72.598	709.103
Dec/24/1998	1588.66	176	212.636	921.739
Nov/9/1999	1589.42	177	134.14	1055.879
Nov/6/1998	1590.6	185	177.366	1233.245

The findings from GEE indicate that the storage capacity of the Koka Reservoir, between the MDDL (1583.7 m.a.s.l) to FRL (1590.6 m.a.s.l), was approximately 1233 Mm^3 during the 1998-1999 period. As a result, sediment deposition in the study area caused a loss of 417 Mm^3 i.e 25.3 % of its live storage capacity. The results of the bathymetric study of year 1999, showed that the storage capacity was 1186.2 Mm^3 with a loss of 463.8 Mm^3 and the original capacity at the impoundment of the dam was 1650 Mm^3. Hence, by assuming a uniform rate of silt deposition the average silt deposition rate in the Koka reservoir is 11 Mm^3 $year^{-1}$ using GEE and 12.2 Mm^3 $year^{-1}$ using bathymetry survey, within a period of 38 years (from 1960 to 1998). Therefore, the percentage annual sedimentation loss of the reservoir in 1998/1999 was 0.9 % $year^{-1}$ using GEE and 1 % $year^{-1}$ using a bathymetry survey. Figure 4-4 shows a comparison of the initial capacity, the cumulative revised capacity based on bathymetry results, and the cumulative revised capacity using GEE-based analysis for the year 1998-1999. It is clear from the graph that the result obtained from GEE shows an agreement with the 1999 bathymetry survey.

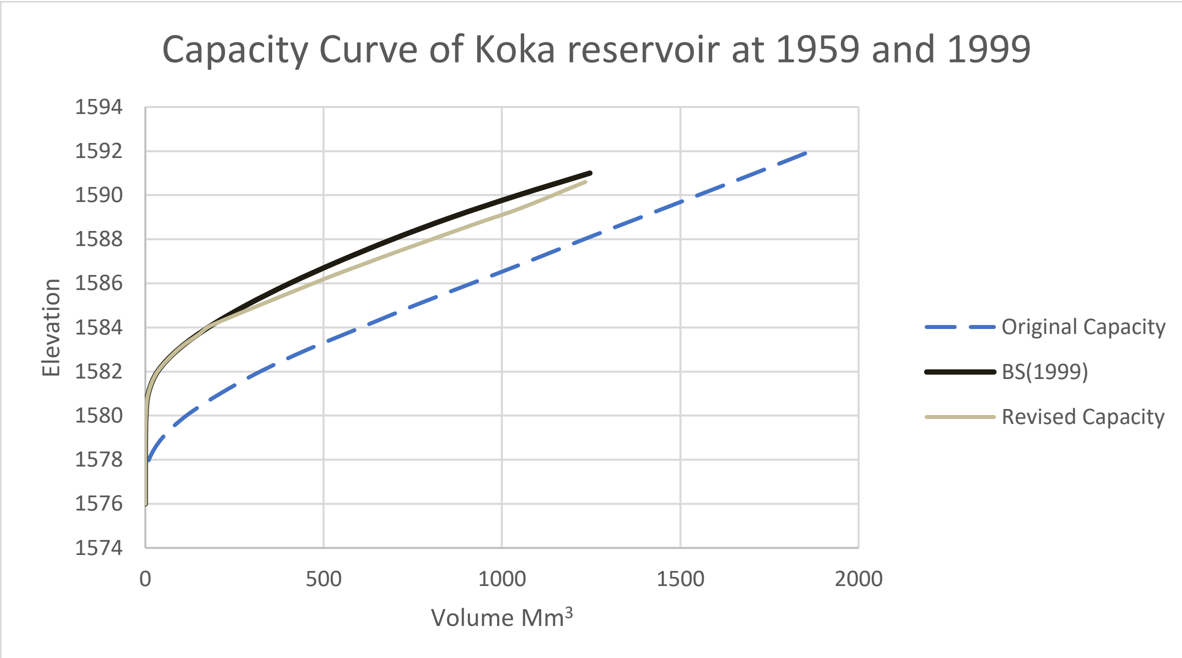

Figure 4-4 A storage curve of the original capacity, cumulative revised (bathymetry result) and cumulative revised (GEE-based) capacities obtained for the year 1998-1999

4.1.1.1 P-test and T-test results

The t-Test is a statistical test used to determine whether there is a significant difference between the means of two groups. In the given results, two variables are there: GEE result and bathymetry survey result. The mean for GEE result is 336.635625, while the mean for bathymetry survey result is 343.6009141. The variances for GEE result and bathymetry survey result are 175396.3202 and 185479.799, respectively. Both variables have 16 observations. The Pearson correlation between the two variables is 0.995485196.

The t-Test results provide us with the t Statistic, which in this case is -0.662319595. The P(T<=t) one-tail value is 0.258906981, and the t Critical one-tail value is 1.753050356. The P(T<=t) two-tail value is 0.517813962, and the t Critical two-tail value is 2.131449546. The P-value is the probability of obtaining a test statistic as extreme as the one observed, assuming the null hypothesis is true. In this case, the P(T<=t) one-tail value is 0.258906981, which is greater than the significance level of 0.05. Therefore, it indicates that there is a close correspondence between the variables. The P(T<=t) two-tail value is 0.517813962, which is also greater than the significance level of 0.05. This indicates that there is a close correspondence between the bathymetry survey result and GEE result.

Table 4-2 P-test and T-test results

t-Test: Paired Two Sample for Means		
	Variable 1	Variable 2
Mean	336.635625	343.6009141
Variance	175396.3202	185479.799
Observations	16	16
Pearson Correlation	0.995485196	
Hypothesized Mean Difference	0	
df	15	
t Stat	-0.662319595	
P(T<=t) one-tail	0.258906981	
t Critical one-tail	1.753050356	
P(T<=t) two-tail	0.517813962	
t Critical two-tail	2.131449546	

4.1.2 Reservoir sedimentation of Koka reservoir at 2021/2022

From the analysis, the outcome demonstrates that GEE worked well in estimating reservoir sedimentation for the year 1998/1999. As a result, the current study was done for the year 2021–2022 using a similar procedure. The cumulative revised capacity of the reservoir at the lowest observed level (1583.54 m.a.s.l) was assumed to be the same as the 1999 bathymetry data cumulative capacity (150.917 Mm^3). The cumulative capacities above the MDDL to the FSL were added up to estimate the cumulative revised capacities. Table 4-2 displays the approximate volume on various dates, which was utilized to determine sediment accumulation in the reservoir.

Table 4-3 Area and cumulative volume obtained from koka reservoir using GEE for the year 2021/2022

Date of satellite pass	Elevation	Area (Km^2)	Volume (Mm^3)	Cumulative Volume (Mm^3)
Jun/01/2022	1583.54	79	134.035	134.035
May/29/2021	1585.23	115	162.981	297.016
May/13/2021	1585.61	119	44.458	341.474
Mar/26/2021	1586.63	131	127.451	468.925
Feb/25/2022	1587.58	140	128.701	597.626
Dec/26/2022	1588.94	150	128.7	726.326
Nov/21/2021	1589.99	161	197.161	923.487
Sep/21/2022	1590.7	179	120.644	1044.131

The Koka reservoir's storage capacity between the MDDL (1583.54 m.a.s.l) and the FSL (1590.7 m.a.s.l) was estimated to be 1044 Mm^3 in 2021-2022. This was compared to the original live storage capacity of 1650 Mm3, resulting in a loss of 606 Mm^3 i.e 36.7% of its live storage capacity. The average annual loss of live storage over 60 years (1960-2021) was 10.1 Mm^3 per year, or 0.97%. To develop the revised area-elevation-capacity curve for 2021/2022, storage capacities and area estimates for different durations were plotted against their respective elevations, as shown in the Figure 4-5.

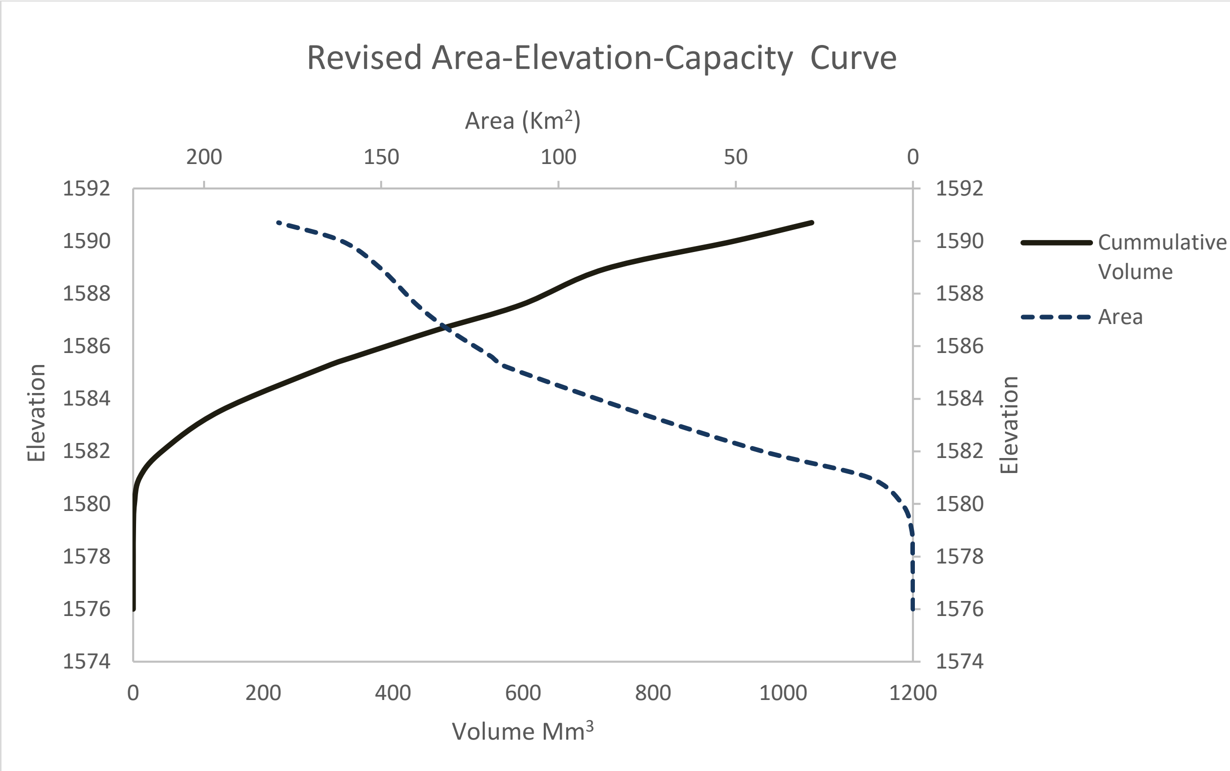

Figure 4-5 Revised area-elevation-capacity curve of koka reservoir for 2021/2022

The comparison between the current findings and the design can be seen in Figure 4-6, which presents the difference in water storage capacity due to sediment accumulation in the reservoir between the water years 1960 and 2021/2022.

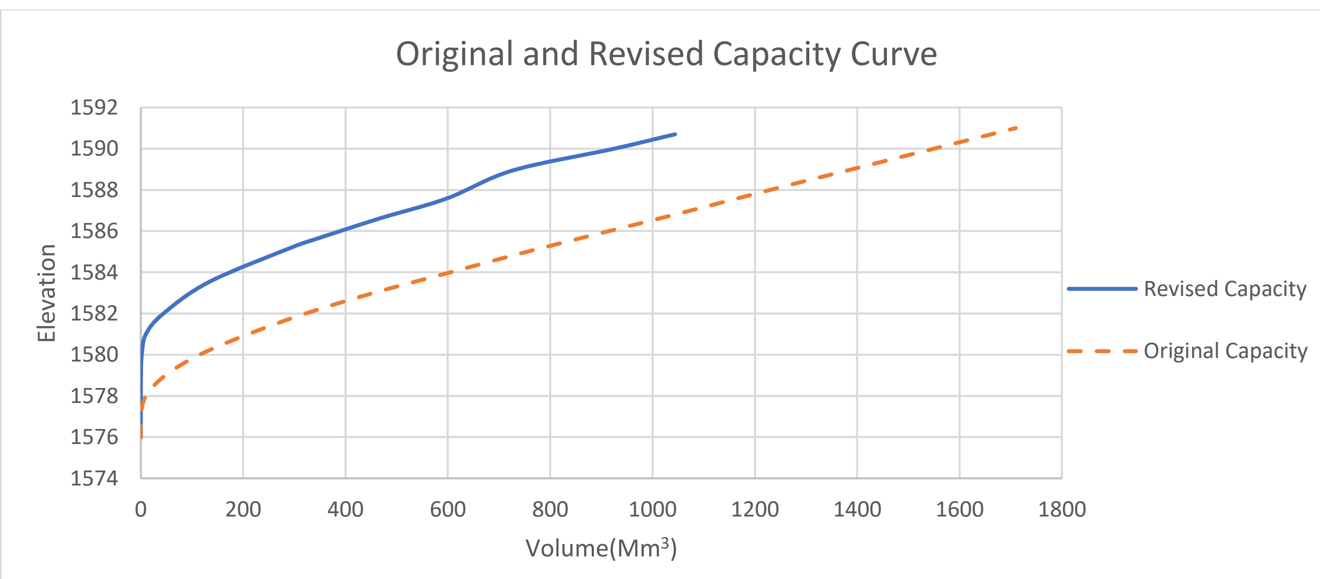

Figure 4-6The comparison of the current findings with the design capacity

4.1.3 Reservoir sedimentation of Gefersa I/II reservoir for the year 2021/2022

The same method used for analyzing Koka reservoir in 2021/2022 was applied to the Gefersa I/II reservoir analysis for the year 2021/2022. The cumulative revised capacity of the reservoir at the lowest observed level (2580.80 m.a.s.l) was assumed to be the same as the 2017 bathymetry data cumulative capacity (0.833). Table 4-3 displays the estimated volume at various dates, which are utilized to calculate sediment accumulation in the reservoir.

Table 4-3Area and cumulative volume obtained from Gefersa I/II reservoir using GEE for the year 2021/2022

Date of satellite pass	Elevation m.a.s. l	Revised Area (Km^2)	Cumulative Volume (Mm^3)
Jun_24_2022	2580.01	0.401	0.833
May_16_2022	2581.27	0.619	1.108
May_29_2021	2582.72	0.771	2.258
Mar_13_2022	2583.41	0.941	2.932
Feb_09_2022	2584.47	1.038	4.126
Jan_21_2021	2585.67	1.198	5.967
Nov_21_2021	2586.61	1.321	7.315
Oct_20_2021	2587.11	1.389	8.102

The storage capacity of the Gefersa I/II reservoir for 2021/2022 was estimated to be 8.102 Mm^3, measured between the MDDL (2580.01 m.a.s.l) to the FSL (2587.11 m.a.s.l). The original capacity of the reservoir, according to the ECDSWC (2017) Bathymetric survey report, is 8.5 Mm^3. This implies that, there has been a decrease of 0.398 Mm^3 i.e 4.7% of its live storage capacity. A comparison of these findings with the bathymetry survey can be seen in Figure 4-8.

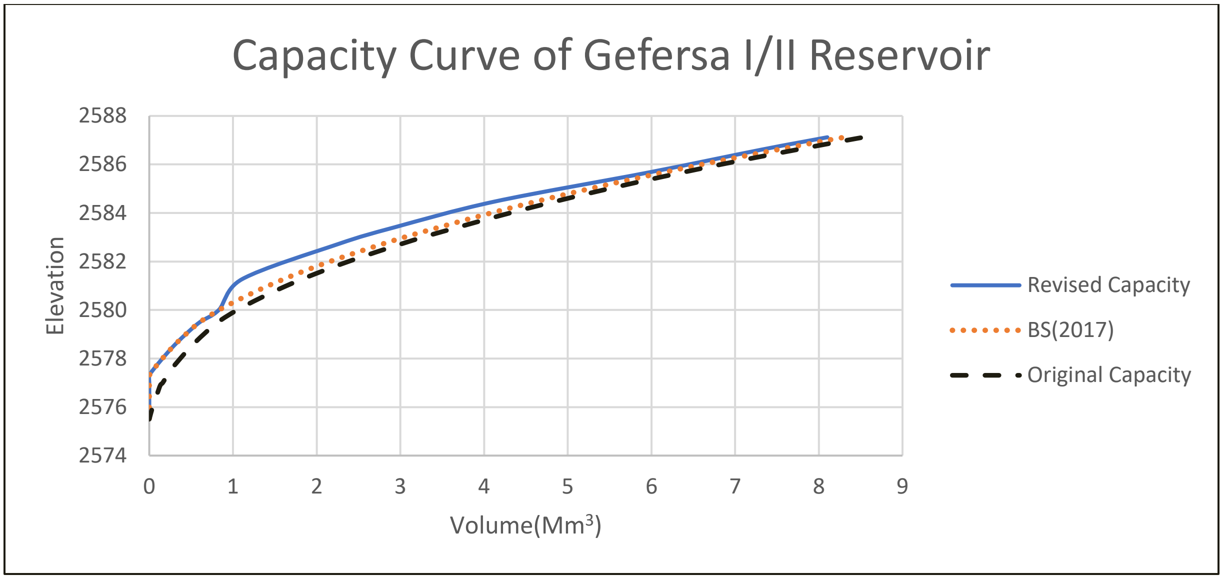

Figure 4-7 Curves of the revised capacity, original capacity and bathymetry survey result

As shown in Figure 4-8 the present revised capacity of the reservoir was compared with the 2017 Bathymetric survey of the Gefersa I/II reservoir and the original capacity of the reservoir. The Bathymetric survey indicates that the total sediment load including bed load, which is deposited in the Gefersa I/II reservoir in 50 years is 0.22 Mm^3 and a total capacity of 8.25 Mm^3. Therefore, by assuming a uniform rate of silt deposition the average silt deposition rate in the Gefersa I/II reservoir is 0.007 Mm^3 $year^{-1}$ using GEE and 0.004 Mm^3 $year^{-1}$ using bathymetry survey, within a period of 55 years and 50 years respectively. Accordingly, the percentage annual sedimentation loss of the reservoir in 2021/2022 is 0.08 % $year^{-1}$ using GEE and 0.05 % $year^{-1}$ using a bathymetry survey. Hence, the estimated storage capacities for various durations were plotted against their respective elevations to develop revised area-elevation-capacity curve, as illustrated in Figure 4-9 for the year 2021/2022.

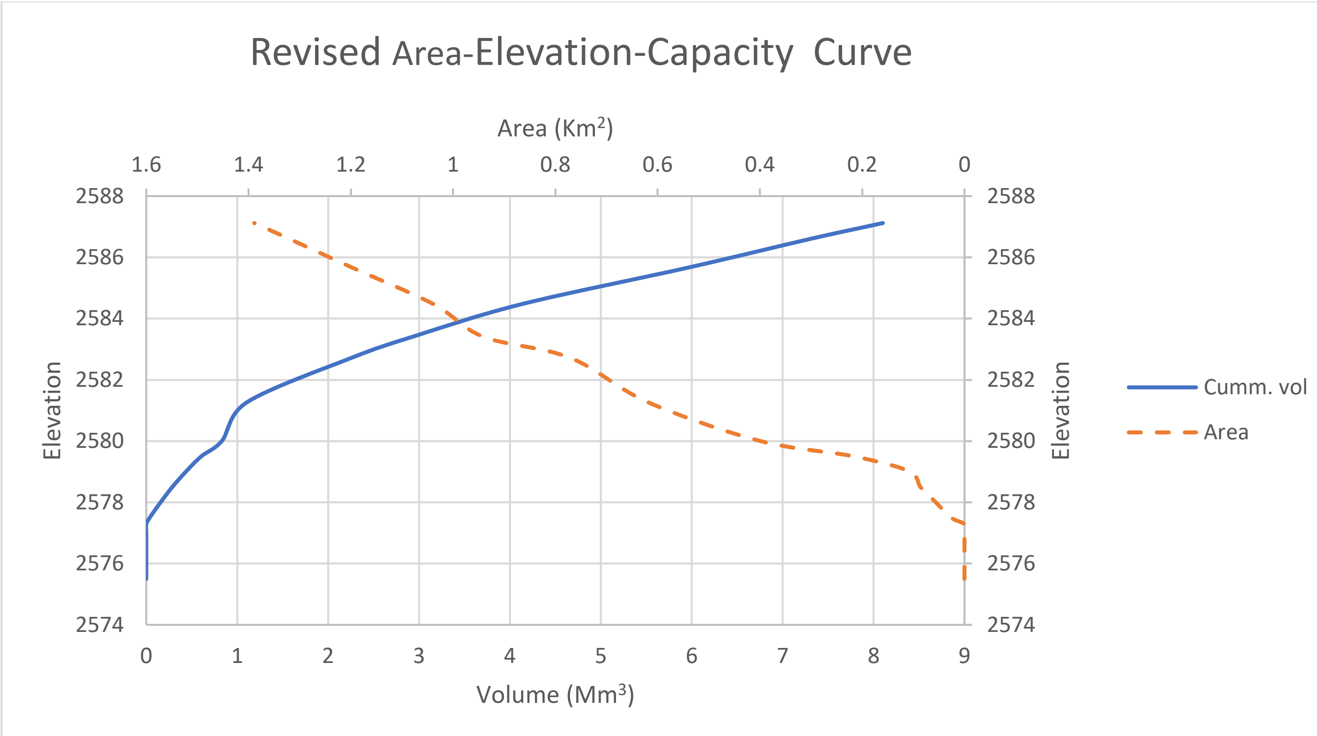

Figure 4-8 Revised area-elevation-capacity curve of Gefersa I/II reservoir

4.1.3.1 P-test and T-test results

The t-Test is a statistical test used to determine whether there is a significant difference between the means of two groups. In the given results, we have two variables: GEE result and bathymetry survey result. The mean for GEE result is 3.20741104, while the mean for bathymetry survey result is 3.249571429. The variances for GEE result and bathymetry survey result are 8.255046481 and 7.594542357, respectively. Both variables have 21 observations. The Pearson correlation between the two variables is 0.985093542.

The t-Test results provide us with the t Statistic, which in this case is -0.386541929. The P(T<=t) one-tail value is 0.35158859, and the t Critical one-tail value is 1.724718243. The P(T<=t) two-tail value is 0.703177179, and the t Critical two-tail value is 2.085963447. To interpret these results, the P-values must be compared to the significance level (usually 0.05). The P(T<=t) one-tail value of 0.35158859 is greater than the significance level, indicating that there is there is a close correspondence between the bathymetry survey result and GEE result. Similarly, the P(T<=t) two-tail value of 0.703177179 is also greater than the significance level, further supporting the lack of evidence for a significant difference between the means of the two variables.

Table 4-4 P-test and T-test results

t-Test: Paired Two Sample for Means		
	Variable 1	*Variable 2*
Mean	3.207411	3.249571
Variance	8.255046	7.594542
Observations	21	21
Pearson Correlation	0.985094	
Hypothesized Mean Difference	0	
df	20	
t Stat	-0.38654	
P(T<=t) one-tail	0.351589	
t Critical one-tail	1.724718	
P(T<=t) two-tail	0.703177	
t Critical two-tail	2.085963	

4.2 Discussion

In the case of the Koka reservoir, the annual sedimentation loss of the reservoir for the year 1998/1999 was 11 Mm^3 $year^{-1}$ (0.9 %) using GEE and 12.2 Mm^3 $year^{-1}$ (1 %) using a bathymetry survey. The findings of the study for the year 1998/1999 show that there is a close correspondence between GEE and bathymetry survey results. As a result, the current study was done for the year 2021–2022 utilizing GEE. Similarly, for the case of Gefersa I/II reservoir the annual sedimentation loss of the reservoir in 1998/1999 was 0.007 Mm^3 $year^{-1}$ using GEE and 0.004 Mm^3 $year^{-1}$ using bathymetry survey. Comparatively, the result of the Gefersa I/II reservoir shows a very close correspondence between GEE and bathymetry survey results than the Koka reservoir. In addition to emphasizing the correlation, P-test and T-test were conducted to determine whether there is a significant difference between the results of GEE and bathymetry survey results. The results of both tests showed a very close correspondence between the two variables for both reservoirs.

Based on the findings from the Koka reservoir in 1998/1999, there is a minor change in the sedimentation rate obtained from GEE. This small shift in sedimentation rate may be due to an underestimation of the reservoir's water spread area. Avinash & Chandramouli (2018) suggest that estimating sedimentation through remote sensing is greatly influenced by the precision in distinguishing between land and water pixels. Similarly, Pandey et al. (2016) stated that determining the water spread area, which is highly sensitive for the estimation of sedimentation using remote sensing. However, if the water level information is exact and the water-spread area is interpreted precisely, it is possible to determine the revised area-elevation-capacity curves quite precisely. In addition, slight differences in the elevation may also impact these results of sedimentation rate. For the present study (Koka reservoir 1998/1999) using GEE the elevation of 1590.6 m.a.s.l was considered as FSL which was a bit lower than the original FSL (1590.7 m.a.s.l). However, despite the slight changes in the annual sediment rate, the findings discovered that the rate of sedimentation found from GEE is in agreement with the results of the bathymetry.

Besides, the results of the Koka Reservoir for the years 1999 and 2021/2022 were compared. The annual sedimentation rate of the present year seems to be lower, compared to the 1999 bathymetry. According to the MoWE bathymetry survey report (1999), before the 1999 survey, three bathymetry surveys has been conducted in 1973, 1981, and 1988. The Koka reservoir experienced yearly silt deposition of 10, 17, 16.8, and 12.2 Mm^3, respectively, according to bathymetry measurements conducted in 1973, 1981, 1988, and 1999. It is obvious from this pattern that the yearly sedimentation rate of the Koka reservoir began to decline from 1981. Similar to this, the current survey's findings indicate that 10.1 Mm^3 of silt is deposited annually, which shows a reduction from the 1999 yearly sediment rate. This sedimentation rates may be decreasing due to highly increased urbanization in the Upper Awash River basin, which includes major cities like Addis Ababa, Bishoftu, and Adama. According to Shawul & Chakma (2019), from 1972 to 2014 the urban area in the basin was expanded by 606.2%. This leads to changes in land use, drainage patterns, and stormwater management infrastructure, which potentially can reduce sediment transport. However, it is essential to note that urbanization can also lead to increased sedimentation rates if not managed properly. Therefore, for further understanding the underlying cause, it is recommended to conduct additional research on this trend of sedimentation rate. Figure 4-10 shows the trend of sedimentation of Koka reservoir for different periods.

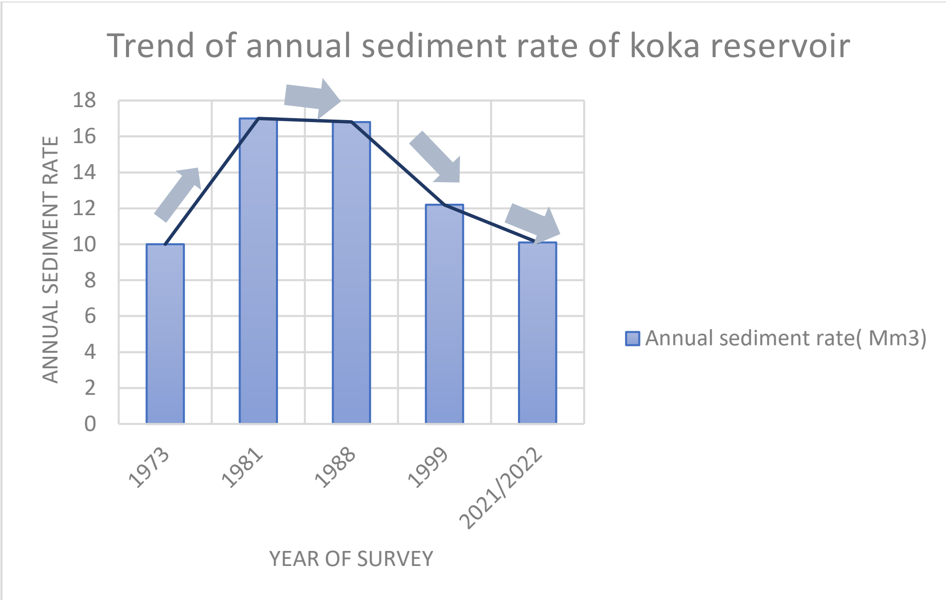

Figure 4-9 Trend of annual sediment rate of Koka reservoir

The annual rate of sedimentation for both reservoir falls within the acceptable global average rate of 1% suggested by Schleiss et al. (2013). However, when compared to the Gefersa I/II reservoir, the Koka reservoir has much greater yearly sedimentation rate. One of the main factors contributing to this difference is the presence of the Gefersa III dam, which is located upstream of the Gefersa I/II reservoir. According to a report by ECDSWC (2017), the construction of the Gefersa III dam has led to a substantial decrease in the sedimentation rate of the Gefersa I/II reservoir, with a reduction of more than 50%. Therefore, this has resulted in a comparatively lower annual sedimentation rate for the Gefersa I/II reservoir.

Furthermore, an effort was made to compare the present results with relevant articles on reservoir sedimentation using remote sensing techniques. However, only a few studies tried to compare the output with a bathymetry survey. A study by Foteh et al. (2018) assessed reservoir sedimentation on Jayakwadi reservoir using a remote sensing technique and compared the findings with the hydrographic survey. The result revealed that sedimentation rate was slightly increased at 5.58 Mm^3 per year compared to the 4.84 Mm^3 per year estimated back in 2012-2013.To support their result, the authors mentioned that the slight variation is caused by sensitivity in the estimation of the water spread area using remote sensing techniques and the varying elevation taken into account by both approaches for FSL had an impact on the outcome. In addition, a study by Tesfaye et al. (2022) studied reservoir sedimentation through remote sensing and GIS techniques, calibrating the methodology in three reservoirs within the Upper Blue Nile Basin: Koga, Shina, and Selamko. The findings revealed an annual storage loss of 0.27 Mm^3 $year^{-1}$ for the Koga reservoir using satellite remote sensing, and 0.20 Mm^3 $year^{-1}$ using bathymetric survey techniques. Similarly, For Shina and Selamko reservoirs, annual storage loss due to sediment depositions is found to be 1.26Mm^3 and 1.03Mm^3 $year^{-1}$ using satellite remote sensing and 1.09Mm^3 and 0.80Mm^3 using bathymetric survey methods, respectively. Thus, the authors concluded that there is a strong correlation between remote sensing techniques and the findings of bathymetry surveys.

In addition, Merina and Ninija (2016) carried out a reservoir sedimentation assessment for the Vaigai reservoir. Using sedimentation reports from 1958 and 2000, they calculated the reduction in storage capacity and compared the annual sedimentation rates. The revised capacity was compared to recent surveys, revealing an overall sediment yield of 32.164 Mm^3, higher than the 2000 yield of 28.252 Mm^3. The average annual silting rates for 1958, 2000, and 2012 were 8.519%, 14.504%, and 16.512%, respectively, indicating a steady increase in the Vaigai Reservoir's silting rate. Similarly, Pandey et al. (2016) studied reservoir sedimentation in Patratu Reservoir, finding its live storage capacity reduced by 11.76% (0.4720 hm^3/year). Comparing this rate to the designed sedimentation rate, they concluded that it was higher than expected. Therefore, it is evident that the outcomes derived from remote sensing techniques exhibit minor discrepancies when compared to the bathymetry survey results.

In general, for the present study GEE performed greatly for the estimation of reservoir sedimentation. The integrated system also offers massive potential by providing high-resolution satellite data and advanced geospatial analysis capabilities, enabling to assess the sedimentation in near-real time. The outcomes of this study will contribute to better understanding and provide insights to encourage its broader usage in the reservoir sedimentation assessment.

Furthermore, Earth Engine is also made to make it simple for scientists to share their findings with other scientists, policymakers, NGOs, field workers, and even the general public(Amani et al., 2020b). Accordingly, the code developed for the present study is uploaded on GitHub and accessible through the provided link in the previous chapter. This ensures that users, regardless of their programming expertise, can access and utilize the code for studying reservoir sedimentation in other contexts. In addition, it has an important implication for the periodic assessment of reservoir sedimentation, especially in developing countries where resources are often limited.

In inference, this research paper demonstrates how GEE can be used to estimate reservoir sedimentation in a timely and accurate manner, which can contribute to achieving the SDGs related to water, climate, and land. The application of GEE in the assessment of reservoir sedimentation is closely related to the Sustainable Development Goals (SDGs). The first SDG that is related to this topic is SDG 6: Clean Water and Sanitation. This goal aims to ensure availability and sustainable management of water and sanitation for all. (Hák et al., 2016). Reservoir sedimentation is a major threat to water security, as it reduces the storage capacity and lifespan of reservoirs, affects water quality and quantity, and increases the risk of flooding and dam failure. By using Google Earth Engine (GEE) to estimate reservoir sedimentation, this paper provides a useful tool for monitoring and managing water resources more effectively and efficiently.

Another SDG that is related to this topic is SDG 13: Climate Action. This goal aims to take urgent action to combat climate change and its impacts. Climate change is expected to exacerbate the problem of reservoir sedimentation, as it can alter the hydrological cycle, increase soil erosion, and intensify extreme weather events(Katila et al., 2019). By using GEE to assess reservoir sedimentation in near-real time, this paper can help identify the areas and periods most vulnerable to sedimentation and inform adaptation strategies.

The next SDG that is related to this topic is SDG 15: Life on Land. This goal aims to protect, restore and promote sustainable use of terrestrial ecosystems, combat desertification, halt and reverse land degradation and halt biodiversity loss(Sayer et al., 2019). Reservoir sedimentation is closely linked to land degradation and biodiversity loss, as it can result from deforestation, overgrazing, mining, agriculture, and urbanization. By using GEE to estimate reservoir sedimentation, this paper can help evaluate the impacts of land use and land cover changes on sedimentation and provide evidence for implementing sustainable land management practices.

However, beyond the advantages of GEE for reservoir sedimentation assessment, it comes with certain limitations. For sedimentation assessment, GEE relies on remote sensing data, which means it can only determine the sedimentation rate within the zone of fluctuation of reservoir water level. In the current research, it is assumed that the volume of reservoirs below the lowest observed level remains unchanged before and after sedimentation. This assumption makes it difficult to accurately determine the sedimentation rate for the entire reservoir. In addition, for the dead load zone, the information on the capacity could only be taken from the bathymetric survey. Therefore, it is recommended to conduct a bathymetry survey at 10 years interval to obtain full reservoir information.

5 CONCLUSION AND RECOMMENDATION

5.1 Conclusion

Reservoir sedimentation occurs on a global scale and is the process of sand and sediment being transported to, deposited in, and accumulating in reservoirs. This process has the potential to cause major economic loss with possible negative consequences on water availability, power generation, water supply, flood control, and others. Thus, a critical assessment of sediment disposition at each of the major and medium reservoirs is necessary to undertake appropriate measures.

This study employed Google Earth Engine, a cloud-based platform, as a remote sensing tool to evaluate reservoir sedimentation. The GEE platform provides an Application Programming Interface (API) through the internet, which offers computational resources and satellite imagery. Thus, an automated methodology was developed using the JavaScript API found in GEE, which enables obtaining and processing satellite imagery. The developed code is intended to acquire and process Landsat images, as well as automatically compute and map the water spread area of the reservoir.

The methodology was applied on Koka and Gefersa I/II reservoirs to determine sediment deposition. To examine the capabilities of Google Earth Engine (GEE) in assessing reservoir sedimentation, a comparison was made with recent bathymetry survey results. For the case of Koka reservoir, due to the constraint of up-to-date bathymetry surveys sedimentation study was conducted for the year 1998/1999, to enable validation of the methodology while bringing it into line with the existing bathymetric survey results of 1999.

From the analysis, the outcome demonstrates that GEE worked well in estimating reservoir sedimentation for the year 1998/1999. In addition, the result revealed that the rate of sedimentation obtained from GEE is in agreement with the results of the bathymetry. As a result, the current study was done for the year 2021–2022 using a similar procedure. The Koka reservoir's storage capacity for the 2021-2022 period was estimated to be 1044 Mm^3 between the lowest water level (1583.54 m.a.s.l) and the full supply level (1590.7 m.a.s.l). It was then compared to the original live storage capacity, and there is a loss of 606 Mm^3 live storage capacity. Hence, the average annual loss was 10.1 Mm^3 $year^{-1}$(0.97 %) within a period of 60 years (from 1960 to 2021).

Similarly, for Gefersa I/II reservoir the same methodology was applied. Thus, the storage capacity between the lowest water level observed during the period of analysis 2580.01 m.a.s.l and FSL 2587.11 m.a.s.l was estimated to be 8.102 Mm^3 for the year 2021/2022. It was then compared to the original live storage capacity, and there is a loss of 0.398 Mm^3 live storage capacity. Therefore, by assuming a uniform rate of silt deposition the average silt deposition rate in the Gefersa I/II reservoir is 0.007 Mm^3 $year^{-1}$ using GEE and 0.004 Mm^3 $year^{-1}$ using bathymetry survey, in live storage within a period of 55 years and 50 years respectively. Comparatively, the result of the Gefersa I/II reservoir shows a very close correspondence between GEE and bathymetry survey results than the Koka reservoir.

For the present study, GEE performed greatly for the estimation of reservoir sedimentation. The integrated system also offers massive potential by providing high-resolution satellite data and advanced geospatial analysis capabilities, enabling to assess the sedimentation in near-real time. The outcomes of this study contribute to better understanding and provide insights to encourage its broader usage in the reservoir sedimentation assessment and can contribute to achieve the SDGs related to water, climate, and land. In addition, it has an important implication for the active management of reservoir sedimentation, especially in developing countries where resources are often limited. To facilitate future sedimentation studies at various reservoirs, the code developed for this study has been uploaded and can be accessed through the link provided in the third chapter. This will make it easier to conduct future sedimentation studies for scientists, policymakers, NGOs, field workers, and even the general public.

5.2 Recommendation

- It is recommended that researchers and policymakers consider using Google Earth Engine (GEE) for timely and accurate estimation of reservoir sedimentation, which can contribute to achieving Sustainable Development Goals (SDGs) related to water, climate, and land.
- It is recommended to explore the potential of the integrated system used in this study, which combines high-resolution satellite data and advanced geospatial analysis capabilities, for assessing sedimentation in near-real time.
- Utilizing the code developed for this study, which is available on GitHub, is recommended to facilitate the broader usage of GEE in reservoir sedimentation assessment.

- It is recommended to conduct a bathymetry survey at 10-year intervals to obtain full reservoir information and improve the accuracy of sedimentation rate determination for the entire reservoir.
- Researchers are advised to consider the limitations of GEE for sedimentation assessment, such as its reliance on remote sensing data and assumptions made regarding the volume of reservoirs below the lowest observed level.
- Evaluating the impacts of land use and land cover changes on sedimentation and utilizing evidence-based approaches for sustainable land management practices are crucial recommendations.
- Researchers and policymakers are encouraged to identify the areas and periods most vulnerable to sedimentation and inform adaptation strategies using GEE to manage water resources more effectively and efficiently.

REFERENCES

Acharya, T. D., Subedi, A., & Lee, D. H. (2018). Evaluation of Water Indices for Surface Water Extraction in a Landsat 8 Scene of Nepal. *Sensors*, *18*(8), 8. https://doi.org/10.3390/s18082580

Adugna, T. M., & Cherie, D. A. (2021). A Review on Reservoirs Sedimenation Problems in Ethiopia. *Asian Journal of Advanced Research and Reports*, 1–8. https://doi.org/10.9734/ajarr/2021/v15i330372

Amani, M., Ghorbanian, A., Ahmadi, S. A., Kakooei, M., Moghimi, A., Mirmazloumi, S. M., Moghaddam, S. H. A., Mahdavi, S., Ghahremanloo, M., Parsian, S., Wu, Q., & Brisco, B. (2020a). Google Earth Engine Cloud Computing Platform for Remote Sensing Big Data Applications: A Comprehensive Review. *IEEE Journal of Selected Topics in Applied Earth Observations and Remote Sensing*, *13*, 5326–5350. https://doi.org/10.1109/JSTARS.2020.3021052

Amani, M., Ghorbanian, A., Ahmadi, S. A., Kakooei, M., Moghimi, A., Mirmazloumi, S. M., Moghaddam, S. H. A., Mahdavi, S., Ghahremanloo, M., Parsian, S., Wu, Q., & Brisco, B. (2020b). Google Earth Engine Cloud Computing Platform for Remote Sensing Big Data Applications: A Comprehensive Review. *IEEE Journal of Selected Topics in Applied Earth Observations and Remote Sensing*, *13*, 5326–5350. https://doi.org/10.1109/JSTARS.2020.3021052

Avinash, G., & Chandramouli, D. P. N. (2018). *Assessment of Reservoir Sedimentation using RS and GIS techniques—A case study of Kabini Reservoir, Karnataka, India*. *05*(08), 6.

Chen, X., Zhao, X., Zhao, Y., Wang, R., Lu, J., Zhuang, H., & Bai, L. (2023). Interaction of Climate Change and Anthropogenic Activity on the Spatiotemporal Changes of Surface

Water Area in Horqin Sandy Land, China. *Remote Sensing*, *15*(7), 7. https://doi.org/10.3390/rs15071918

Chi, M., Plaza, A., Benediktsson, J. A., Sun, Z., Shen, J., & Zhu, Y. (2016). Big Data for Remote Sensing: Challenges and Opportunities. *Proceedings of the IEEE*, *104*(11), 2207–2219. https://doi.org/10.1109/JPROC.2016.2598228

Condeça, J., Nascimento, J., & Barreiras, N. (2022a). Monitoring the Storage Volume of Water Reservoirs Using Google Earth Engine. *Water Resources Research*, *58*(3), e2021WR030026. https://doi.org/10.1029/2021WR030026

Condeça, J., Nascimento, J., & Barreiras, N. (2022b). *Monitoring the Storage Volume of Water Reservoirs Using Google Earth Engine—Condeça—2022—Water Resources Research—Wiley Online Library*. https://agupubs.onlinelibrary.wiley.com/doi/full/10.1029/2021WR030026

Dutta, S. (2016). Soil erosion, sediment yield and sedimentation of reservoir: A review. *Modeling Earth Systems and Environment*, *2*(3), 123. https://doi.org/10.1007/s40808-016-0182-y

ECDSWC, 2018 Gefersa Intake Rehabilitation and Bathymetric Survey Work Project Final Detail Design Report (With Out Dam Heightening).

Feyisa, G. L., Meilby, H., Fensholt, R., & Proud, S. R. (2014). Automated Water Extraction Index: A new technique for surface water mapping using Landsat imagery. *Remote Sensing of Environment*, *140*, 23–35. https://doi.org/10.1016/j.rse.2013.08.029

Foteh, R., Garg, V., Nikam, B. R., Khadatare, M. Y., Aggarwal, S. P., & Kumar, A. S. (2018). Reservoir Sedimentation Assessment Through Remote Sensing and Hydrological Modelling. *Journal of the Indian Society of Remote Sensing*, *46*(11), 11. https://doi.org/10.1007/s12524-018-0843-6

Frost, J. (2017, April 18). *Interpreting P values*. Statistics By Jim. http://statisticsbyjim.com/hypothesis-testing/interpreting-p-values/

Gao, H. (2015). Satellite remote sensing of large lakes and reservoirs: From elevation and area to storage. *WIREs Water*, *2*(2), 147–157. https://doi.org/10.1002/wat2.1065

Geleta, H. I. (2011). *Watershed sediment yield modeling for data scarce areas* [DoctoralThesis]. http://elib.uni-stuttgart.de/handle/11682/375

Gorelick, N., Hancher, M., Dixon, M., Ilyushchenko, S., Thau, D., & Moore, R. (2017). Google Earth Engine: Planetary-scale geospatial analysis for everyone. *Remote Sensing of Environment*, *202*, 18–27. https://doi.org/10.1016/j.rse.2017.06.031

Gurmu, Z. A., Ritzema, H., Fraiture, C. de, Riksen, M., & Ayana, M. (2021). Sediment Influx and Its Drivers in Farmers' Managed Irrigation Schemes in Ethiopia. *Water*, *13*(13), 13. https://doi.org/10.3390/w13131747

Hák, T., Janoušková, S., & Moldan, B. (2016). Sustainable Development Goals: A need for relevant indicators. *Ecological Indicators*, *60*, 565–573. https://doi.org/10.1016/j.ecolind.2015.08.003

Haregeweyn, N., Poesen, J., Nyssen, J., De Wit, J., Haile, M., Govers, G., & Deckers, S. (2006). Reservoirs in Tigray (Northern Ethiopia): Characteristics and sediment deposition problems. *Land Degradation & Development*, *17*(2), 211–230. https://doi.org/10.1002/ldr.698

JAIN, S. K., SINGH, P., & SETH, S. M. (2002). Assessment of sedimentation in Bhakra Reservoir in the western Himalayan region using remotely sensed data. *Hydrological Sciences Journal*, *47*(2), 203–212. https://doi.org/10.1080/02626660209492924

Jain, S. K., & Singh, V. P. (2003). *Water resources system planning and management*.

Katila, P., Colfer, C. J. P., Jong, W. de, Galloway, G., Pacheco, P., & Winkel, G. (2019). *Sustainable Development Goals*. Cambridge University Press.

Kumar, L., & Mutanga, O. (2018). Google Earth Engine Applications Since Inception: Usage, Trends, and Potential. *Remote Sensing*, *10*(10), 10. https://doi.org/10.3390/rs10101509

Liu, Z., Yao, Z., & Wang, R. (2016). Assessing methods of identifying open water bodies using Landsat 8 OLI imagery. *Environmental Earth Sciences*, *75*(10), 873. https://doi.org/10.1007/s12665-016-5686-2

Mamo, S. (2002). Water balance evaluation, leakage rate and total water loss of Koka Reservoir, Ethiopia: Comments on previous studies and new determinations. *SINET: Ethiopian Journal of Science*, *25*(1), 1. https://doi.org/10.4314/sinet.v25i1.18077

McFEETERS, S. K. (1996). The use of the Normalized Difference Water Index (NDWI) in the delineation of open water features. *International Journal of Remote Sensing*, *17*(7), 1425–1432. https://doi.org/10.1080/01431169608948714

MoWE. Koka Dam Bathymetry Survey Report. 1999.

Moges, M. M., Abay, D., & Engidayehu, H. (2018). Investigating reservoir sedimentation and its implications to watershed sediment yield: The case of two small dams in data-scarce upper Blue Nile Basin, Ethiopia. *Lakes & Reservoirs: Science, Policy and Management for Sustainable Use*, *23*(3), 217–229. https://doi.org/10.1111/lre.12234

Mohammad, E.-A. (2020). *Sedimentation and Its Challenge for Sustainability of Hydraulic Structures: A Case Study of Mosul Dam Pumping Station*. https://www.diva-portal.org/smash/record.jsf?pid=diva2%3A1397009&dswid=-4630

Negm, A., Elsahabi, M., & Ali, K. (2017). A Satellite Remote Sensing Approach to Estimate the Lifetime Span of Aswan High Dam Reservoir. In A. M. Negm (Ed.), *The Nile River* (pp. 57–77). Springer International Publishing. https://doi.org/10.1007/698_2017_15

Nghia, B. P. Q., Pal, I., Chollacoop, N., & Mukhopadhyay, A. (2022). Applying Google earth engine for flood mapping and monitoring in the downstream provinces of Mekong river. *Progress in Disaster Science*, *14*, 100235. https://doi.org/10.1016/j.pdisas.2022.100235

Ninija Merina, R. (2016). Sedimentation study in a reservoir using remote sensing technique. *Applied Ecology and Environmental Research*, *14*(4), 296–304. https://doi.org/10.15666/aeer/1404_296304

Obialor, C., Okeke, O., Onunkwo, A., & Fagorite, V. (2019). Reservoir sedimentation: causes, effects and mitigation. 2488–9849.

Pandey, A., Chaube, U. C., Mishra, S. K., & Kumar, D. (2016). Assessment of reservoir sedimentation using remote sensing and recommendations for desilting Patratu Reservoir, India. *Hydrological Sciences Journal*, *61*(4), 711–718. https://doi.org/10.1080/02626667.2014.993988

Pekel, J.-F., Cottam, A., Gorelick, N., & Belward, A. S. (2016). High-resolution mapping of global surface water and its long-term changes. *Nature*, *540*(7633), 418–422. https://doi.org/10.1038/nature20584

Perera, D., Williams, S., & Smakhtin, V. (2023). Present and Future Losses of Storage in Large Reservoirs Due to Sedimentation: A Country-Wise Global Assessment. *Sustainability*, *15*(1), 1. https://doi.org/10.3390/su15010219

Rohi, D., & Bisri, M. (2013). *The Impact of Sedimentation in Reservoirs on Performance Operation of Hydropower: A Case Study Sutami Hydropower Indonesia*. *4*(1).

Sayer, J., Sheil, D., Galloway, G., Riggs, R. A., Mewett, G., MacDicken, K. G., Arts, B. J. M., Boedhihartono, A. K., Langston, J., & Edwards, D. P. (2019). SDG 15 Life on Land – The Central Role of Forests in Sustainable Development. In *Sustainable Development*

Goals: Their Impacts on Forest and People (pp. 482–509). Cambridge University Press. https://doi.org/10.1017/9781108765015.017

Schleiss, A. J. (2013). Sedimentation of Reservoirs. In P. T. Bobrowsky (Ed.), *Encyclopedia of Natural Hazards* (pp. 901–905). Springer Netherlands. https://doi.org/10.1007/978-1-4020-4399-4_312

Singh, S., Dhasmana, M. K., Shrivastava, V., Sharma, V., Pokhriyal, N., Thakur, P. K., Aggarwal, S. P., Nikam, B. R., Garg, V., Chouksey, A., & Dhote, P. R. (2018). Estimation Of Revised Capacity In Gobind Sagar Reservoir Using Google Earth Engine And Gis. *The International Archives of the Photogrammetry, Remote Sensing and Spatial Information Sciences*, *XLII–5*, 589–595. https://doi.org/10.5194/isprs-archives-XLII-5-589-2018

Sumi, T., & Hirose, T. (2009). *Accumulation of Sediment in Reservoirs*.

Tamiminia, H., Salehi, B., Mahdianpari, M., Quackenbush, L., Adeli, S., & Brisco, B. (2020). Google Earth Engine for geo-big data applications: A meta-analysis and systematic review. *ISPRS Journal of Photogrammetry and Remote Sensing*, *164*, 152–170. https://doi.org/10.1016/j.isprsjprs.2020.04.001

Tesfaye, A. T., Moges, M. A., Moges, M. M., Worqlul, A. W., Defersha, D. T., & Wassie, A. B. (2022). Reservoir sedimentation evaluation using remote sensing and GIS approaches for the reservoirs in the upper Blue Nile Basin. *Sustainable Water Resources Management*, *9*(1), 23. https://doi.org/10.1007/s40899-022-00792-0

Tew, Y. L., Tan, M. L., Samat, N., Chan, N. W., Mahamud, M., Sabjan, M., Lee, L. K., See, K., & Wee, S. (2022). Comparison of Three Water Indices for Tropical Aquaculture Ponds

Extraction using Google Earth Engine. *Sains Malaysiana*, *51*, 369–378. https://doi.org/10.17576/jsm-2022-5102-04

Tsegaye, L., & Bharti, R. (2021). Soil erosion and sediment yield assessment using RUSLE and GIS-based approach in Anjeb watershed, Northwest Ethiopia. *SN Applied Sciences*, *3*(5), 582. https://doi.org/10.1007/s42452-021-04564-x

USGS. United States Geological Survey, Landsat 8 Quality Assessment Band [Internet]. 2014. Available from: https://landsat.usgs.gov/L8QualityAssessmentBand. php

Wagh, S., & Manekar, V. (2021). Assessment of Reservoir Sedimentation using Satellite Remote Sensing Technique (SRS). *Journal of The Institution of Engineers (India): Series A*, *102*(3), 851–860. https://doi.org/10.1007/s40030-021-00539-8

Xu, H. (2006). Modification of normalised difference water index (NDWI) to enhance open water features in remotely sensed imagery. *International Journal of Remote Sensing*, *27*(14), 3025–3033. https://doi.org/10.1080/01431160600589179

Zhai, K., Wu, X., Qin, Y., & Du, P. (2015). Comparison of surface water extraction performances of different classic water indices using OLI and TM imageries in different situations. *Geo-Spatial Information Science*, *18*(1), 1. https://doi.org/10.1080/10095020.2015.1017911

Zhang, C., Dong, J., Xie, Y., Zhang, X., & Ge, Q. (2022). Mapping irrigated croplands in China using a synergetic training sample generating method, machine learning classifier, and Google Earth Engine. *International Journal of Applied Earth Observation and Geoinformation*, *112*, 102888. https://doi.org/10.1016/j.jag.2022.102888

Zhe, Z., Shixiong, W., & Curtis, E. W. (2015). Improvement and expansion of the Fmask algorithm: Cloud, cloud shadow, and snow detection for Landsats 4–7, 8, and Sentinel 2 images. *Remote Sensing of Environment*, *159*, 269–277.

https://doi.org/10.1016/j.rse.2014.12.014

Appendices

Table 6-0-1Original capacity and bathymetry survey of koka reservoir

Elevation m.a.s.l.	ΔS Mm^3	
	1959 survey	1999 survey
1577	0	0
1578	10	0.02
1579	38	0.18
1580	67	1.4
1581	95	6.5
1582	112	26.1
1583	133	57.6
1584	150	84.4
1585	150	106.0
1586	160	122.6
1587	160	137.8
1588	160	150.5
1589	160	166.2
1590	160	186.1
1591	160	201.1

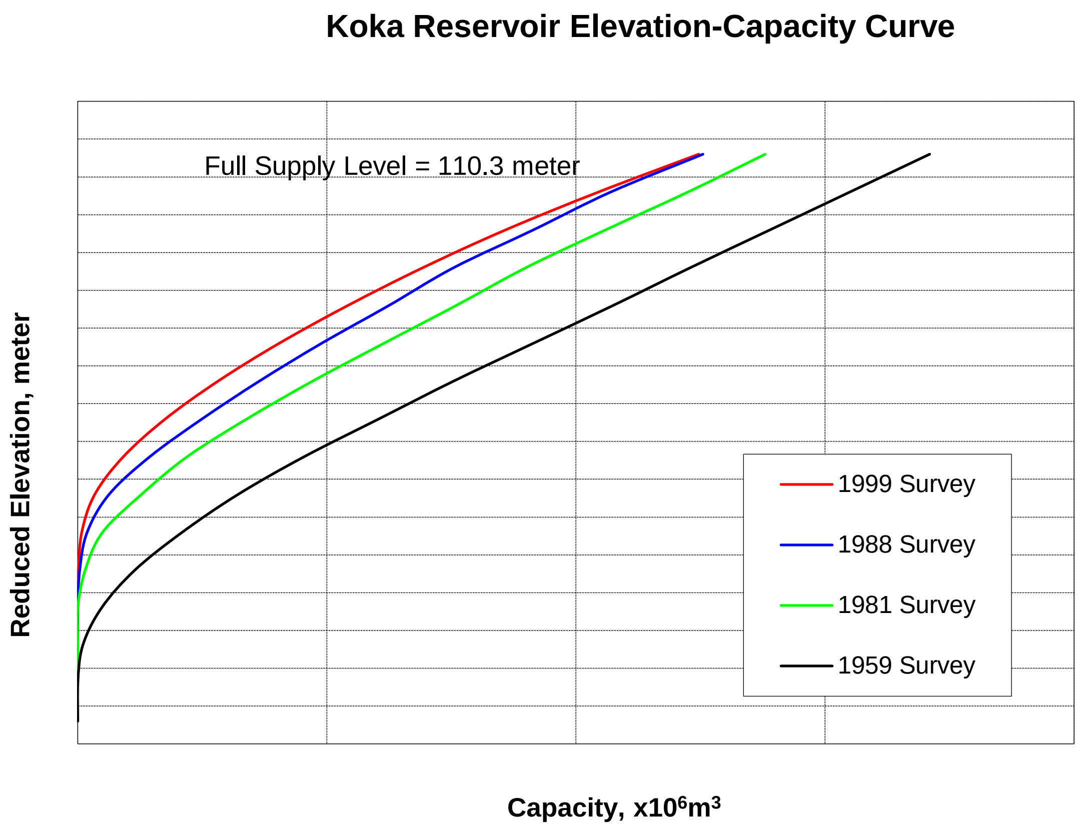

Figure 6-0-1 capacity curve of recent bathymetry survey of koka reservoir

Table 6-0-2 Original capacity and bathymetry survey of Gefersa I/II reservoir

Elevation m.a.s.l	Original Area Km²	Original Capacity Mm³	Revised Area Km²	Modified Revised Capacity Mm³
2589	1.89	11.82	1.696	11.585
2588.5	1.82	10.9	1.626	10.666
2588	1.74	10.01	1.546	9.777
2587.5	1.67	9.15	1.476	8.918
2587.1	1.598	8.50	1.404	8.271
2587	1.58	8.34	1.386	8.109
2586.5	1.51	7.57	1.316	7.340
2586	1.42	6.83	1.226	6.601
2585.5	1.34	6.14	1.146	5.912
2585	1.26	5.49	1.066	5.263
2584.5	1.18	4.88	0.986	4.654
2584	1.1	4.31	0.906	4.085
2583.5	1.03	3.78	0.836	3.556
2583	0.97	3.27	0.776	3.047

Elevation m.a.s.l	Original Area Km²	Original Capacity Mm³	Revised Area Km²	Modified Revised Capacity Mm³
2582.5	0.9	2.81	0.706	2.588
2582	0.82	2.38	0.626	2.159
2581.5	0.73	1.99	0.536	1.770
2581	0.66	1.64	0.466	1.421
2580.5	0.59	1.33	0.396	1.112
2580	0.51	1.05	0.316	0.833
2579.5	0.41	0.82	0.216	0.604
2579	0.3	0.65	0.106	0.435
2578.5	0.28	0.5	0.086	0.286
2578	0.25	0.37	0.056	0.157
2577.5	0.22	0.25	0.026	0.038
2577.287	0.19	0.212	0.000	0.000
2577	0.16	0.16	0.000	0.000
2576.9	0.144	0.132	0.000	0.000
2576.5	0.12	0.09	0.000	0.000
2576	0.09	0.04	0.000	0.000
2575.5	0.06	0	0.000	0.000

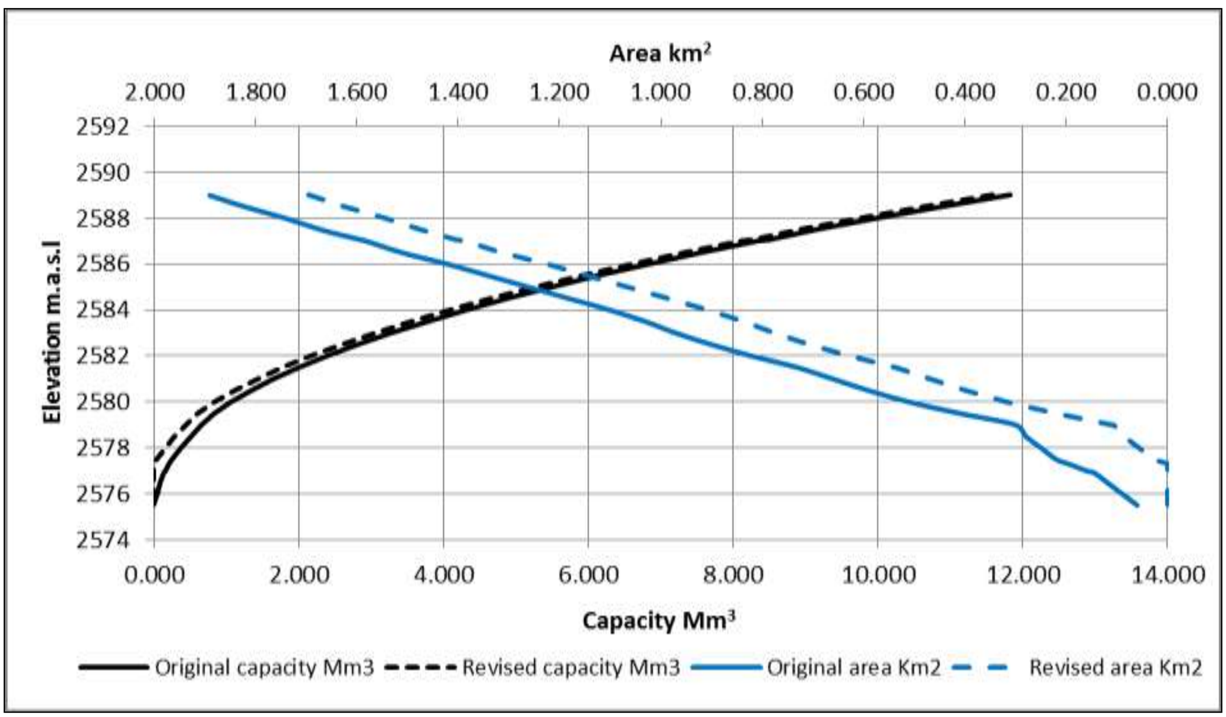

Figure 6-0-2 Original and bathymetry survey Area capacity curve of Gefersa I/II reservoir